Multiplex, single-cell CRISPRa screening for cell type specific regulatory elements

Florence M. Chardon[1,†], Troy A. McDiarmid[1,†], Nicholas F. Page[2,3,4], Beth Martin[1], Silvia Domcke[1], Samuel G. Regalado[1], Jean-Benoît Lalanne[1], Diego Calderon[1], Lea M. Starita[1,5], Stephan J. Sanders[2,4,6], Nadav Ahituv[3,4,*], and Jay Shendure[1,5,7,8,*]

Affiliations:
1. Department of Genome Sciences, University of Washington, Seattle, WA, USA
2. Department of Psychiatry and Behavioral Sciences, Kavli Institute for Fundamental Neuroscience, Weill Institute for Neurosciences, University of California, San Francisco, San Francisco, CA, USA
3. Department of Bioengineering and Therapeutic Sciences, University of California, San Francisco, San Francisco, CA, USA
4. Institute for Human Genetics, University of California, San Francisco, San Francisco, CA, USA
5. Brotman Baty Institute for Precision Medicine, Seattle, WA, USA
6. Institute of Developmental and Regenerative Medicine, Department of Paediatrics, University of Oxford, Oxford, OX3 7TY, UK
7. Howard Hughes Medical Institute, Seattle, WA, USA
8. Allen Discovery Center for Cell Lineage Tracing, Seattle, WA, USA

†. These authors contributed equally to this work

* Correspondence to N.A. (Nadav.Ahituv@ucsf.edu) or J.S. (shendure@uw.edu)

Abstract

CRISPR-based gene activation (CRISPRa) is a promising therapeutic approach for gene therapy, upregulating gene expression by targeting promoters or enhancers in a tissue/cell-type specific manner. Here, we describe an experimental framework that combines highly multiplexed perturbations with single-cell RNA sequencing (sc-RNA-seq) to identify cell-type-specific, CRISPRa-responsive *cis*-regulatory elements and the gene(s) they regulate. Random combinations of many gRNAs are introduced to each of many cells, which are then profiled and partitioned into test and control groups to test for effect(s) of CRISPRa perturbations of both enhancers and promoters on the expression of neighboring genes. Applying this method to candidate *cis*-regulatory elements in both K562 cells and iPSC-derived excitatory neurons, we identify gRNAs capable of specifically and potently upregulating target genes, including autism spectrum disorder (ASD) and neurodevelopmental disorder (NDD) risk genes. A consistent pattern is that the responsiveness of individual enhancers to CRISPRa is restricted by cell type, implying a dependency on either chromatin landscape and/or additional *trans*-acting factors for successful gene activation. The approach outlined here may facilitate large-scale screens for gRNAs that activate therapeutically relevant genes in a cell type-specific manner.

Introduction

There are millions of candidate *cis*-regulatory elements (cCREs) in the human genome, yet only a handful have been functionally validated and confidently linked to their target gene(s)[1]. Recently, we and others have combined CRISPR-interference (CRISPRi) and sc-RNA-seq to scalably validate distal cCREs, while also linking them to the gene(s) that they regulate[1–4]. However, to date, the vast majority of work in the field has focused on screening candidate regulatory elements for *necessity*, with only a few studies screening for *sufficiency* in the endogenous context.

CRISPR-activation (CRISPRa) is a versatile approach that allows one to test for the sufficiency of cCRE activity[5–8]. CRISPRa screens of noncoding regulatory elements have at least four potential advantages over CRISPRi screens. First, as noted above, CRISPRa can identify cCREs that are sufficient even if not singularly necessary to drive target gene expression. Second, CRISPRa can identify elements that, when targeted, may upregulate already active genes above their baseline levels. Third, CRISPRa has the potential to discover inactive regions that, when transcriptional activation machinery is recruited to them, can act as active enhancers and increase expression of nearby genes[9]. Finally, CRISPRa has the potential to identify cCRE-targeting gRNAs whose activity is cell type-specific, opening the door to "*cis* regulatory therapy" (CRT) for haploinsufficient and other low-dosage associated disorders, as recently demonstrated for monogenic forms of obesity and autism spectrum disorder[10,11]. However, despite these potential advantages, CRISPRa targeting of noncoding regulatory elements has mostly been deployed in an *ad hoc* manner[9,12–14], and typically in workhorse cancer cell lines rather than more therapeutically relevant *in vitro* models.

Here, we present a scalable framework in which we introduce multiple, random combinations of CRISPRa perturbations to each of many cells followed by sc-RNA-seq (**Fig. 1**), analogous to an approach that we previously developed for CRISPRi screening[2]. Computational partitioning of cells into test and control groups based on detected gRNAs enables greater power than single-plex CRISPRa screens, as any given single-cell transcriptome is informative with respect to multiple perturbations[2]. In this proof-of-concept study, we performed two screens in which the same set of cCREs was targeted, first in K562 cells and then in human iPSC-derived excitatory neurons. We discover both enhancer and promoter-targeting gRNAs capable of mediating upregulation of target gene(s). For enhancers in particular, the upregulatory potential of individual gRNAs was consistently restricted to one cell type, implying a dependency on either the *cis* chromatin landscape and/or additional *trans*-acting factors for successful gene activation.

Results

Multiplex single-cell CRISPRa screening of regulatory elements in K562 cells

As a proof of principle, we first sought to implement multiplex single-cell CRISPRa screening in the chronic myelogenous leukemia cell line K562, an ENCODE Tier 1 cell line[15] in which we had previously performed a multiplex CRISPRi screen[2]. Our proof-of-concept library included gRNAs targeting transcription start site (TSS) positive controls (30 gRNAs), candidate promoters (313 gRNAs), candidate enhancers (100 gRNAs) and non-targeting controls (NTCs; 50 gRNAs). The 30 TSS positive control gRNAs were selected from a previously reported hCRISPRa-v2 library[16], while the 313 candidate promoter-targeting gRNAs were designed to 50 annotated TSSs of 9 high-confidence haploinsufficient risk genes associated with ASD and NDD (*BCL11A*, *TCF4*, *ANK2*, *CHD8*, *TBR1*, *SCN2A*, *SYNGAP1*, *FOXP1*, and *SHANK3*) that are potential therapeutic targets for CRT[17]. The candidate enhancer-targeting guides included 50 gRNAs designed to target 25 enhancer hits previously validated by CRISPRi[2], as well as 50 gRNAs designed to target 25 enhancer "non-hits" (*i.e.* sequences with biochemical markers strongly predictive of enhancer activity in K562 cells that did not alter gene expression when targeted with CRISPRi[2]) (**Fig. S1A-B**; **Methods**). We cloned this gRNA library (n=493) into piggyFlex, a piggyBac transposon-based gRNA expression vector, to allow for genomic integration and stable expression of gRNAs[18]. The piggyFlex vector has both antibiotic (puromycin) and fluorophore (GFP) markers, enabling flexibly stringent selection for cells with higher numbers of gRNA integrants. Additionally, this vector design allows for gRNA transcript capture during single-cell library preparation[18] (**Fig. S1C**).

There is no consensus on which CRISPRa activation complex is best suited for broad and scalable targeting of enhancers[13]. We therefore tested both the VP64 activation complex, which consists of four copies of the VP16 effector, and the VPR activation complex, which consists of the VP64 effector fused to the p65 and Rta effectors[19,20]. The VPR complex has been shown to lead to higher levels of transcriptional activation than that of the VP64 complex. However,

this increased upregulation could achieve higher than therapeutically needed expression levels and being much larger than VP64 could impinge on packaging and delivery of gene therapy vectors such as adeno associated virus (AAV)[20]. We generated a monoclonal, stably VP64-expressing K562 cell line, purchased a polyclonal, stably VPR-expressing K562 cell line (**Fig. 2A**; **Methods**), and validated the capacity of these lines for CRISPRa with a minimal cytomegalovirus (CMV) promoter-tdTomato reporter expression assay[21] (**Fig. S2**).

We then transfected the gRNA library and piggyBac transposase into each cell line at a 20:1 library-to-transposase ratio to achieve high multiplicity of integration (MOI), and selected cells with puromycin. Cells were cultured for nine days before harvesting for sc-RNA-seq to capture and assign gRNAs to single cell transcriptomes (**Fig. 2A**; **Fig. S1**). After QC filtering, we recovered 33,944 high-quality single-cell transcriptomes across the two cell lines, with 79% of cells having one or more detected gRNAs. We recovered a mean of 2.5 gRNAs per cell (**Fig. 2B**) and 178 cells per gRNA (**Fig. 2C**). Transcriptome quality, MOI, gRNA assignment rate, and gRNA coverage were similar across all four sc-RNA-seq batches (10x Genomics lanes) as well as the two cell lines tested (**Fig. S3**).

To systematically assess the effect of each CRISPR perturbation on target gene expression, we adapted an iterative differential expression testing strategy in which all single cell transcriptomes are computationally partitioned into cells with or without a given gRNA[2]. These two groups are then tested for differential expression of all genes within 1 megabase (Mb) (upper estimate of topologically associated domain size in mammalian genomes[22]) upstream and downstream of the gRNA target site (**Fig. 1**; **Fig. 2A**; **Methods**). In both VP64- and VPR-mediated CRISPRa screening experiments, we observed robust upregulation from both promoter and enhancer-targeting gRNAs (276/391 $\log_2$FC>0, 70.6%, $p<2.2\times10^{-16}$, Fisher's Exact Test; **Fig. 2D-E**). The presence of an excess of highly significant *P*-values for cells harboring targeting gRNAs versus non-targeting controls (NTCs) also indicates that this multiplex framework successfully detects upregulation of genes from CRISPRa perturbations (**Fig. 2D**). Effects were consistently much stronger and more significant in the dCas9-VP64 cell line as compared to the dCas9-VPR line (**Fig. S3**). This may be due to differences between the VP64 and VPR effectors, site-of-integration effects (VP64 line is monoclonal while VPR line is polyclonal), MOI differences of the integrated effectors, power differences (more cells were recovered per perturbation for the VP64 line than the VPR line), or a combination of these factors.

To identify significant associations between cCRE-targeting gRNAs and their target genes, which we term "hit gRNAs", we set an empirical false discovery rate (FDR) threshold based on the *P*-values from the NTC gRNA differential expression tests, which are subject to the same sources of noise and error as the targeting gRNA tests. Using an empirical FDR cutoff of 0.1 (**Methods**), we identified 60 activating gRNA hits, including 8 TSS-targeting positive control gRNAs, 40 candidate promoter-targeting gRNAs, 9 distal enhancer hit gRNAs, 2 distal enhancer hit gRNAs wherein the target gene of CRISPRa vs. CRISPRi differed, and 1 distal enhancer non-hit gRNA (in the last three contexts, hit vs. non-hit refers to whether they were "hits" in the previous CRIPSRi-based screen with the same guides and cell line[2]) (**Fig. 2E**; **Fig. S4**). Successfully activating gRNAs were strongly enriched for targeting regions proximal to the genes that they upregulated (**Fig. 2F**) and were specific to their predicted target (45/48 promoter-targeting gRNA hits and 9/12 successful enhancer-targeting gRNAs exclusively upregulated the predicted target and no other gene within 1 Mb; **Fig. S4**; **Table S2**). The gRNAs that upregulated a gene other than the predicted target are discussed further below. Of note, we also observed no instances where targeting a regulatory element, whether a promoter or enhancer, caused significant upregulation of >1 gene.

Taken together, these results demonstrate the potential of this framework to efficiently identify promoter- or enhancer-targeting gRNAs that drive potent, specific upregulation of their target genes in a cell type of interest. Of note, the promoters that were successfully targeted with CRISPRa included genes that were already well-expressed (*e.g., CCND2*, *GNB1*), including two that are haploinsufficient neurodevelopmental disease genes (*FOXP1*, *CHD8*) (**Fig. 2G-H**; **Fig. S4**; **Table S2-S4**). For *CHD8*, in which variants leading to haploinsufficiency are important risk factors for ASD and NDD[23,24], we identified multiple CRISPRa-potent gRNAs targeting distinct isoform-specific promoters, providing an inroad to isoform-specific CRT (**Fig. 2H**; **Fig. S2-S4**).

Our strongest hits were at the promoters of genes with very low or undetectable expression in K562 (*e.g., ANK2*, *BCL11A*; **Fig. 2G**; **Table S2-S4**). For example, we identified multiple CRISPRa-potent gRNAs targeting *ANK2*, an ASD/NDD risk gene with a complex isoform structure[23,24] that is very lowly expressed in K562 cells (**Fig. 2I**). Interestingly, the strongest hits for *ANK2* all targeted a TSS that is not prioritized by biochemical marks (*i.e.*, it is relatively inaccessible and displays a low degree of H3K27ac in K562 cells compared to candidate TSSs of other genes in our library; **Fig. 2I**).

On the other hand, for many targeted TSSs or promoters, only one gRNA, if any, potently activated their target gene when coupled to CRISPRa. More specifically, out of the 313 candidate promoter-targeting gRNAs designed to 50 annotated TSSs of 9 genes, only 38 gRNAs, targeting 10 TSSs and 5 genes, successfully mediated upregulation. An additional 2 gRNAs upregulated different genes (*RPS18* and *WWC3*) than their intended targets (*SYNGAP1* and *FOXP1*). These results underscore the value of inclusive, empirical screens to identify both CRISPRa-competent promoters as well as gRNAs that can successfully activate them.

At the outset of this work, it was unclear if targeting CRISPRa perturbations to enhancers alone (without co-targeting putatively associated promoters) could reliably increase target gene expression to an extent detectable with conventional sc-RNA-seq[9,12,13]. To determine if CRISPRa targeted to a single enhancer alone could effectively upregulate target gene expression, we analyzed our 50 targeted candidate enhancers, 25 of which were previously validated by multiplex CRISPRi in K562 cells[2]. We observed target gene upregulation for 8 of these 50 targeted candidate enhancers (as noted above, mediated by 12 gRNAs; **Fig. 2G**; **Fig. S4**). Six of the 8 enhancers come from the set of 25 enhancer-gene pairs that we also identified with CRISPRi[2], including several cases where distinct gRNAs targeting the same enhancer are both successful, *e.g.* two CRISPRa-competent enhancers of *ANXA1* (**Fig. 2G**; **Fig. S4**). In addition, we identified: (1) an enhancer-targeting gRNA that was not a hit in the CRISPRi screen, but here led to upregulation of *HMGA1*; and (2) two enhancer-targeting gRNAs that mediate downregulation of *TUBA1A* when coupled to CRISPRi, but upregulation of *ASIC1* when coupled to CRISPRa. Taken together, these results show that multiplex CRISPRa screens leveraging sc-RNA-seq can identify enhancer-targeting gRNAs that can mediate potent upregulation of specific genes without co-targeting of the corresponding promoters (**Fig. 2G**; **Fig. S4**; **Table S2-S4**). Furthermore, differences in activity and target-choice despite using the same gRNAs hint at potential differences between CRISPRi and CRISPRa that warrant further exploration.

Multiplex single-cell CRISPRa screening of regulatory elements in post-mitotic iPSC-derived neurons

We next sought to extend this framework beyond K562 cells to a model that is more relevant for native biology as well as CRT, post-mitotic human induced pluripotent stem cell (iPSC)-derived neurons (**Fig. 3A**)[25]. For this, we used a WTC11 iPSC line equipped with a doxycycline-inducible *NGN2* transgene expressed from the *AAVS1* safe-harbor locus to drive neural differentiation, as well as a ecDHFR-dCas9-VPH construct, expressed from the *CLYBL* safe-harbor locus, to drive CRISPRa (**Fig. S5A-B**)[6]. In this line, addition of doxycycline to induce *NGN2* expression and trimethoprim (TMP) to inhibit the ecDHFR degrons drives neural differentiation and initiates CRISPRa[6]. Expression of NGN2 in iPSCs commits these cells to a neuronal fate, and post-mitotic neurons with neuronal morphology develop within days[26].

After optimizing iPSC transfection conditions to achieve high numbers of integrated gRNAs per cell via nucleofection, we integrated the same gRNA library (at a 5:1 gRNA-library:transposase ratio) into iPSCs as we did for the K562 screen (**Fig. 3A**). Following integration, we confirmed functional CRISPRa activity in these neurons via the same tdTomato expression assay used in our K562 CRISPRa validation (**Fig. S5B**). In addition to optimizing transfection conditions, we sought to further boost the multiplicity of gRNA integrations per cell by selecting the cells with a high concentration of puromycin (**Fig. 3A**). After differentiating to neurons over 19 days, we proceeded to sc-RNA-seq. Half of the neurons went directly into sc-RNA-seq (10x Genomics), while the other half were dissociated and flow sorted based on GFP expression (top 40%) prior to sc-RNA-seq, again with the goal of boosting the multiplicity of gRNA integrations (**Fig. 3A**). After quality control filtering, we retained 51,183 single-cell transcriptomes, of which we recovered 1+ associated gRNAs for 89%. With our optimized transfection protocol, we identified a mean of 6.14 gRNAs/cell (**Fig. 3B**) and a mean of 638 cells that harbored each individual gRNA (**Fig. 3C**). Sorting on GFP expression prior to sc-RNA-seq resulted in a 2-fold increase in the number of gRNAs identified per cell (**Fig. S6**).

Our differentiated neurons most closely resemble 14- to 35-day differentiated neurons obtained via *NGN2* induction in iPSCs by an independent group[27] (inferred by integration of these sc-RNA-seq datasets; **Fig. 3D**; **Fig. S7**). A minority of the neurons transcriptionally resemble an intermediate neuronal fate, a difference that we tentatively attribute to the absence of co-cultured glia in our differentiation protocol. Although glia are known to promote maturation of NGN2-induced neurons (and were used in generating the dataset we are comparing to[27]), we excluded them because they can also introduce culture variability due to batch effects introduced by primary glia[26].

We confirmed that the neurons had progressed beyond a pluripotent state and were committed to a post-mitotic neuronal fate by the expression of the pan-neuronal marker *MAP2* and the lack of expression of the pluripotency marker

185 *NANOG* (**Fig. S7**). These neurons also express *LHX9* and *GPM6A* -- markers of central nervous system (CNS) neurons
186 (**Fig. S7C**); and *CUX1* and *SLC17A7*, but not GABAergic markers *GAD1* and *GAD2,* supporting their assignment as
187 excitatory rather than inhibitory neurons (**Fig. S7F**)[25]. Consistent with this, when we co-embedded our transcriptome data
188 onto data from Lin et al.[27], they overlay with "Fate 2" and "Fate 3" cells, which transcriptionally resemble CNS neurons
189 (**Fig. 3D**; **Methods**). Of note, there was no readily apparent enrichment of specific gRNAs within particular clusters (**Fig.**
190 **S8**), which is consistent with the specificity of the observed instances of upregulation (**Fig. S8**).

191 We applied the same differential expression testing strategy as used for the K562 screen to the iPSC-derived neuron
192 screen data, with an empirical FDR cutoff of 0.1 to call significant hits. Similarly to the K562 screen, we observed robust
193 upregulation from targeting gRNAs (281/383 $\log_2$FC>0, 73.4%, $p<2.2\times10^{-16}$, Fisher's Exact Test) and an excess of highly
194 significant *P*-values for targeting gRNA tests compared to NTCs (**Fig. 3E**), confirming that this overall framework is
195 transferable to more physiologically and clinically relevant models such as iPSC-derived neurons. As with the K562
196 screen, we observed strong enrichment for genomic proximity between successful gRNAs and their target genes, but no
197 such enrichment for NTCs tested for associations with target genes randomly selected from the same set (**Fig. S9**).

198 There were 17 hit gRNAs in neurons (FDR < 0.1; **Fig. 3G**), all of which were TSS-targeting positive controls (n = 6)
199 or candidate promoters of ASD/NDD risk genes (n = 11) (**Fig. S10**). Of these 17 hit gRNAs, 12 were also hits in the K562
200 screen while 5 were specific to iPSC-derived neurons (**Fig. S11A**). The screen in iPSC-derived neurons was strikingly
201 target-specific: 16 of 17 of our identified hits, all promoter-targeting gRNAs, upregulated their anticipated target gene and
202 no other genes within the 1-Mb window tested (**Table S5-S7**). The only gRNA hit in iPSC-derived neurons resulting in
203 upregulation of an unintended gene was a gRNA targeting the TSS of the pseudogene *PPP5D1* that led to upregulation
204 of the calmodulin gene *CALM3* (**Fig. S10D**), but this is presumably due to these two genes sharing a bidirectional,
205 outward-oriented core promoter. This gRNA also drove upregulation of *CALM3* in the CRISPRa screen of K562 cells
206 (**Fig. S4D**). We observed no significant differences across several characteristics (*e.g.*, GC content, baseline target gene
207 expression level, the number of cells harboring each gRNA) between gRNAs yielding successful activation and those not
208 in K562 cells and neurons, with the exception that K562 enhancer hit gRNAs tended to have more cells (**Fig. S12**).

209 Similar to K562 cells, we observed several instances where a specific TSS was most amenable to activation (**Fig.**
210 **S13**). One such example is *TCF4*, an ASD/NDD risk gene[23,24]that is a strong candidate for CRT due to its large cDNA
211 size (precluding it from fitting into an AAV) and complex locus architecture. We tested 14 candidate TSSs of *TCF4* and
212 identified 5 gRNAs capable of driving upregulation of *TCF4* in neurons, all of which target the same candidate TSS that
213 resides in open chromatin with strong H3K27ac signal (**Fig. 3H-I**; **Fig. S13A**). Our hits also included examples of cell
214 type-specific promoters. Among these were several gRNAs targeting candidate promoters of ASD/NDD risk genes
215 capable of upregulating genes that are not expressed or rarely expressed in iPSC-derived *NGN2*-differentiated neurons
216 (**Fig. 3H**). For example, gRNAs targeting the promoter of *TBR1*, a transcription factor expressed in forebrain cortical
217 neurons but known not to be expressed in NGN2-differentiated iPSC-derived neurons[25] led to *TBR1* upregulation (**Fig.**
218 **3J**; **Fig. S13B**). Of note, these same gRNAs did not result in upregulation of *TBR1* in K562 cells. This suggests that these
219 neurons are in a permissive state for CRISPRa to activate *TBR1*, despite a lack of highly accessible chromatin in the
220 region targeted by the *TBR1* gRNA (**Fig. 3H, J; Fig. S13B**). Whether these differences in "*TBR1* activatability" are due
221 to differences in the chromatin environment at this locus between K562 cells and iPSC-derived neurons, or alternatively
222 differences in the milieu of *trans*-acting factors, remains an open question.

223 However, in contrast to the cell type-specific promoter examples noted above, we more often observed consistent
224 upregulation across promoter targets and TSS-targeting controls between the two cell types (**Fig. S11**). Specifically, 12
225 out of 17 of the promoter- and TSS-targeting hit gRNAs in neurons were also hits in K562 cells, and upregulation was
226 correlated across cellular contexts (Pearson's correlation coefficient = 0.75, **Fig. S11**). In contrast, we observed striking
227 cell type-specificity for targeted enhancers that were successfully upregulated. While 20% (12/60) of our K562 screening
228 hits were enhancer-targeting gRNAs (**Fig. S4**), none of these were also hits in neurons (**Fig. S10**; **Fig. S14**). Even putting
229 aside significance, the fold-effects on the anticipated target genes of K562-competent activating gRNAs were not well-
230 correlated between cell types (**Fig. 3F**; **Fig. S11B,** Pearson's correlation coefficient = -0.18). Overall, these results show
231 that it is possible to drive cell type-specific upregulation of a gene of interest by targeting CRISPRa to a cell type-specific
232 distal enhancer, without co-targeting of the corresponding promoter.

233

Discussion

Here, we describe a scalable framework for identifying cell-type-specific regulatory elements which when targeted with CRISPRa can drive the upregulation of specific target genes. In applying this framework, we identified gRNAs functionally and cell type-specifically targeting promoters of haploinsufficient genes in K562 cells and iPSC-derived excitatory neurons. We identified a novel candidate enhancer-gene pair that is CRISPRa- but not CRISPRi-sensitive, as well as an instance in which a single enhancer, targeted by the same gRNAs, modulated different genes when coupled to CRISPRa vs. CRISPRi. Our approach holds potential to massively scale the screening for gRNAs and cell-type-specific CREs capable of upregulating remaining functional copies of the roughly 660 genes known to cause disease or disorders when haploinsufficient.

Several of our strongest gRNA hits were not prioritized by typical predictors of enhancer function, such as chromatin accessibility or H3K27ac histone modifications. For example, we are able to upregulate *TBR1* in iPSC-derived neurons by targeting a promoter region that is largely within closed chromatin in this cellular context. Indeed, while measures of proximity, accessibility, and enhancer-related biochemical marks are all strong predictors, none are conclusive or deterministic predictors of regulatory sequence function, either alone or in combination. This underscores the importance of empirical, systematic screens for CRISPRa-responsive regulatory sequences with approaches such as the one described here. Ultimately, a variety of factors including chromatin accessibility and epigenetic modifications, gRNA design quality, and target-specific nuances around CRISPRa-responsiveness, may play a role in determining the success of a CRISPRa perturbation in a given cellular context. Future scaling of this technology and its application to additional, clinically relevant cell types, will provide rich training sets that may enable derivation of rational CRISPRa gRNA design rules for distal, cell-type-specific gene activation, which, in contrast to promoters and CRISPRi[16,28,29], are quite lacking at present. Further, these results illustrate the unique potential of noncoding CRISPRa screens to identify regulatory elements that can mediate upregulation of target genes, regardless of whether or not the gene is natively expressed in the cell type of interest or not.

A major question that we sought to answer through these experiments was whether one can target candidate enhancer sequences with a CRISPRa perturbation and observe upregulation of an intended target gene via scRNA-seq. There have been relatively few efforts to apply CRISPRa to enhancers to date, and most have focused on a handful of enhancer regions and measuring expression of only nearby genes of interest as a readout[9,12,13]. Recent literature suggests that co-targeting a promoter and the candidate enhancer in question can make the enhancer CRISPRa perturbations more efficient and reliable[13]. Although feasible, co-targeting an enhancer and promoter is less likely to yield cell-type-specific upregulation of target genes -- a likely requirement for effective CRT. Delivery of multiple gRNAs also complicates therapeutic delivery and increases the chances of effects on off-target genes (not to mention off-target cell types). Despite using gRNAs that were optimized for CRISPRi screening in our CRISPRa screen, we observed target gene upregulation for 8 of 25 enhancers that we targeted (32%), showing that one can reliably increase target gene expression by targeting enhancers alone. We imagine that this success rate can be improved via a combination of brute force, *i.e.* testing more gRNAs, and better CRISPRa-specific gRNA design.

Multiplex, single-cell CRISPRa screening is a scalable approach to identifying functional CRISPRa gRNAs that can upregulate intended target genes in either a general or cell-type-specific manner. We introduced multiple perturbations per cell, which increased the power of our assay (*i.e.* a mean of 1 gRNA per cell would have required sc-RNA-seq of >400,000 cells to achieve the same power). Given the ease of generating large numbers of differentiated neurons with *in vitro* human neural cultures, sorting on the GFP-positive gRNA expression vector prior to single-cell transcriptome profiling offers a straightforward way to further boost the number of gRNAs captured per cell. In addition, improvements in methods to capture specific transcripts (in this case, gRNAs) with more cost-effective and scalable transcriptional profiling methods such as sci-RNA-seq[30,31] may enable considerably larger screens for a given cost.

CRT is a promising, next-generation therapeutic approach that harnesses endogenous gene regulatory circuits to treat genetic disorders[10,11,17]. However, CRT requires an intricate knowledge of the regulatory elements capable of driving target gene upregulation at physiologically relevant levels specifically in affected tissues. We envision that the framework described here can be deployed in increasingly sophisticated *in vitro* and *in vivo* models of human development to discover reagents capable of treating the hundreds of disorders associated with low gene dosage.

Main text figures

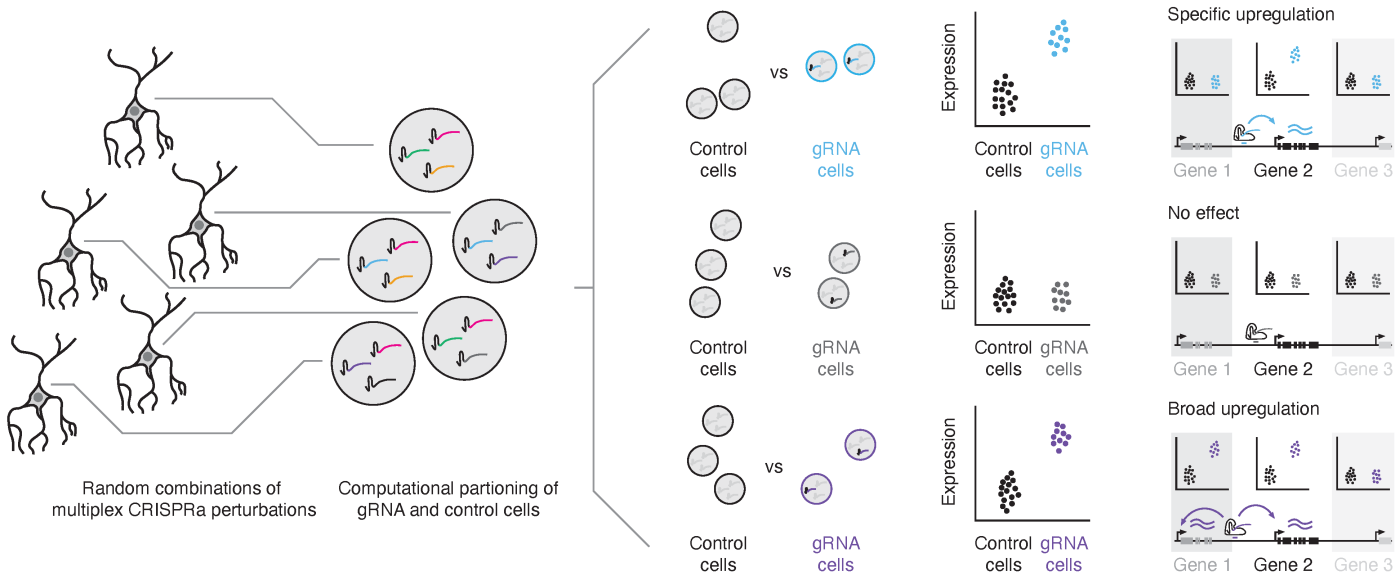

Figure 1 | Multiplex, single cell CRISPRa screening for cell type-specific regulatory elements. (Left) A library of gRNAs targeting candidate cis-regulatory elements (cCREs) is introduced in a multiplex fashion to a population of cells expressing CRISPRa machinery, such that each cell contains a random combination of multiple CRISPRa-mediated perturbations. (Middle) Following single cell transcriptional profiling and gRNA assignment, cells are systematically computationally partitioned into those with or without a given gRNA and tested for upregulation of neighboring genes. (Right) CRISPRa perturbations can either result in target-specific upregulation, no detectable effect (*e.g.*, for non-targeting controls) or, at least theoretically, broad *cis*-upregulation of multiple genes in the vicinity of the gRNA/CRISPRa machinery. Furthermore, patterns of upregulation can either be general or cell type-specific.

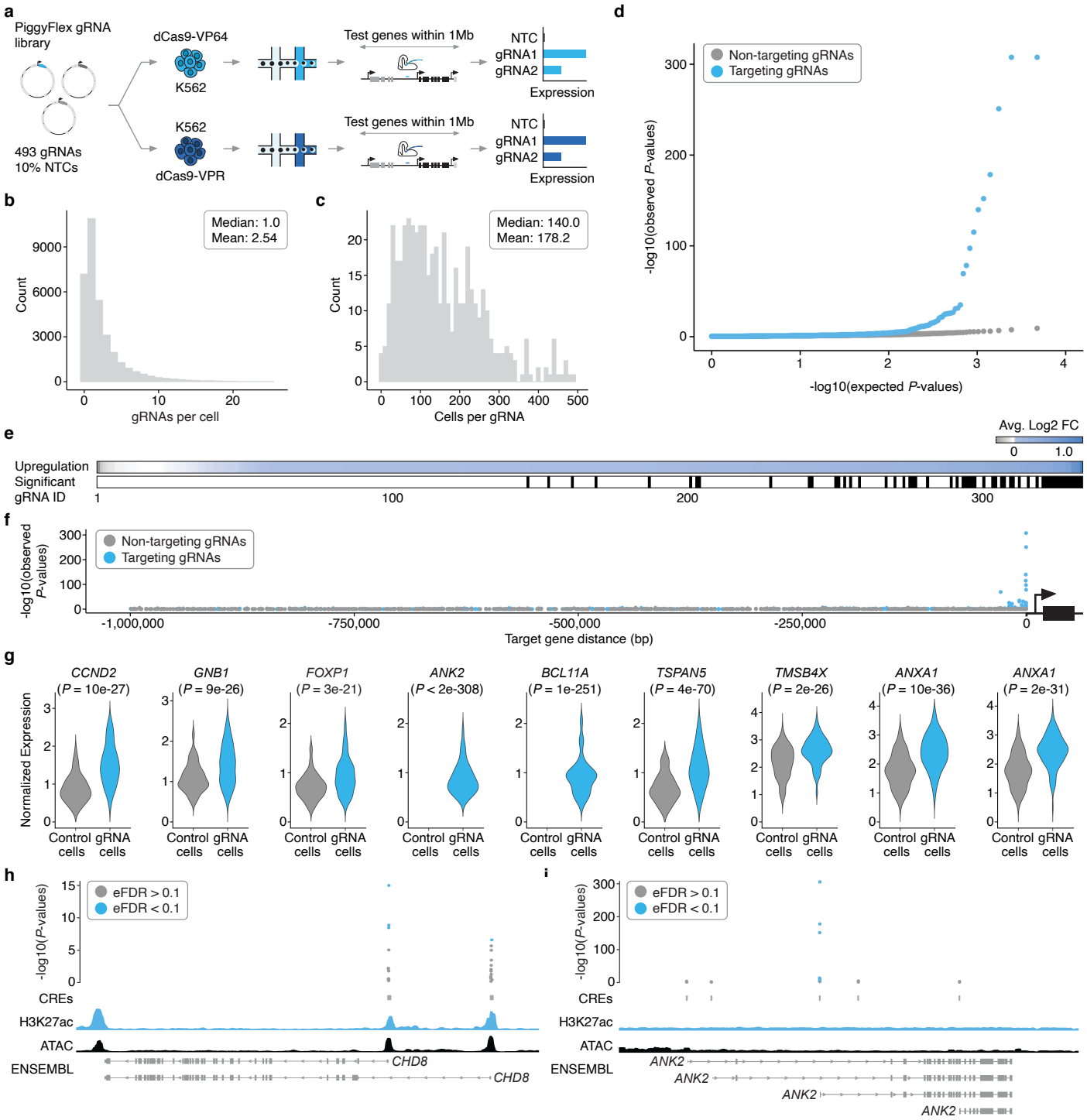

Figure 2 | Multiplex single cell CRISPRa screening of regulatory elements in K562 cells. a) A piggyFlex library containing gRNAs targeting candidate promoters and distal CREs, TSS positive controls, and 10% NTCs was introduced via nucleofection to two K562 cell lines expressing integrated CRISPRa machinery: 1) K562 CRISPRa-VP64 and 2) K562 CRISPRa-VPR. Following selection, 20,000 cells per CRISPRa K562 line (40,000 total) were harvested and profiled using sc-RNA-seq to capture and assign gRNAs to single cell transcriptomes (see **Fig. S1** and methods for details on piggyFlex design and gRNA capture). **b)** Following QC and gRNA assignment, we identified an average of 2.54 gRNAs/cell (median 1.0 gRNAs/cell). **c)** Multiplexing more than one perturbation per cell enabled an average of 178.2 cells/gRNA (median 140.0 cells/gRNA). **d)** Quantile-quantile plot showing the distribution of expected vs. observed *P*-values for targeting (blue) and non-targeting (gray, downsampled) differential expression tests. **e)** (Top) Heatmap showing the average log2 fold change in expression between cells with each targeting gRNA vs. controls for each of the

primary/programmed target genes. Tests are sorted left-to-right by increasing log2 fold change. (Bottom) Categorical heatmap showing which of the perturbations drove significant upregulation using an Empirical FDR approach (EFDR < 0.1). **f)** Targeting gRNAs yielding significant upregulation are enriched for proximity to their target gene. We observe no such enrichment for NTCs tested for associations with target genes randomly selected from the same set. **g)** Example violin plots showing the average log2 fold change between cells with a given gRNA and controls for select hit gRNAs. Hits include TSS positive controls (*CCND2*, *GNB1*), candidate promoters of genes rarely or not expressed in K562 cells (*ANK2*, *BCL11A*) and candidate K562 enhancers (*TSPAN5*, *TMSB4X*, and *ANXA1*). Control cells are downsampled to have the same number of cells as the average number of cells detected per gRNA (n = 178) for visualization. **h)** Hits included multiple gRNAs targeting isoform-specific promoters of *CHD8*. Empirical *P*-values are visualized alongside tracks for K562 ATAC-seq (ENCODE), H3K27ac signal (ENCODE), and RefSeq validated transcripts (ENSEMBL/NCBI) **i)** The strongest hit gRNAs for ANK2 target the same promoter that is not prioritized by biochemical marks (*e.g.*, accessibility or H3K27ac). Genomic tracks are the same as in panel **h**. Abbreviations: NTC: Non-targeting controls.

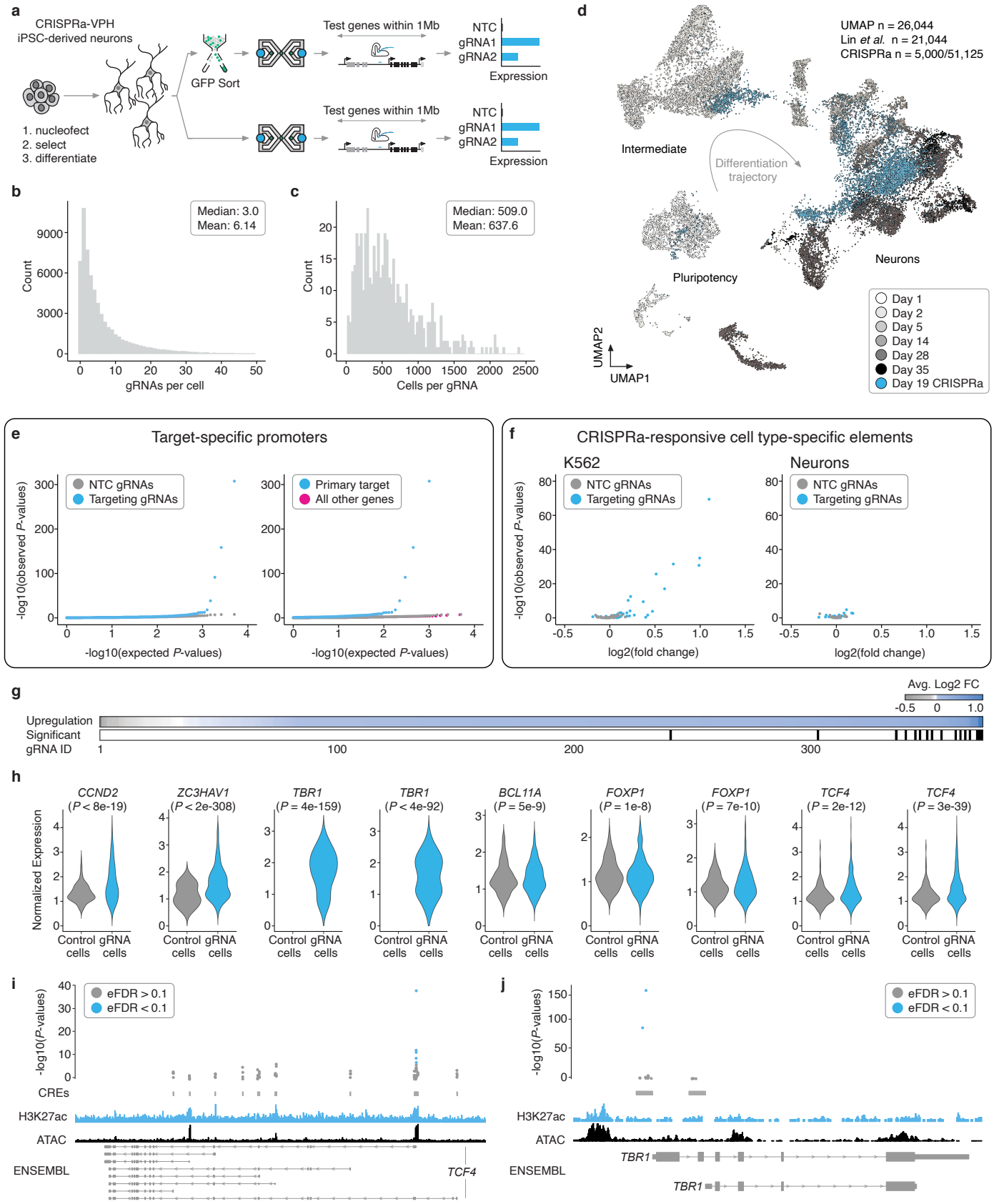

Figure 3 | Multiplex single cell CRISPRa screening of regulatory elements in post-mitotic iPSC-derived neurons. **a)** The same piggyFlex library as used in K562 experiments was introduced to a human WTC11 iPSC line harboring TMP-inducible CRISPRa machinery and a Dox-inducible NGN2 transgene to drive neural differentiation. Following

selection and differentiation, cells were harvested and profiled with sc-RNA-seq to capture gRNAs and assign them to single cell transcriptomes. Half of the neurons were sorted on GFP immediately prior to sc-RNA-seq to increase the multiplicity of gRNA integrations. **b)** Following QC and gRNA assignment, we identified an average of 6.14 gRNAs/cell (median 3.0). **c)** Neuron gRNA coverage: each gRNA was identified in an average of 637.6 cells (median 509.0). **d)** UMAP projection of the neuron dataset from this study (blue, 51,183 cells downsampled to 5,000 cells to aid with visualization) onto a sc-RNA-seq differentiation time-course from a similar differentiation protocol and NGN2 iPSC line (21,044 cells)[25]. This reference time-course dataset is coloured from white to black based on differentiation day. **e)** (Left) QQ-plot displaying observed vs. expected *P*-value distributions for targeting (blue) and NTC (downsampled) populations. (Right) QQ-plot for targeting tests against their intended/programmed target (blue) compared to targeting tests of all other genes with 1Mb of each gRNA (pink) and NTCs (gray downsampled). There is a clear excess of highly significant *P*-values for programmed targets compared to targeting tests of neighboring genes (pink) or NTCs (gray). **f)** Volcano plot showing the average log2 fold change and *P*-values exclusively for gRNAs that target putative enhancers in K562 cells (left) and iPSC-derived neurons (right). **g)** (Top) Heatmap showing the average log2 fold change in expression between cells with each targeting gRNA vs. controls for each of the primary/programmed target genes. (Bottom) Categorical heatmap showing which of the perturbations produced significant upregulation using an Empirical FDR approach (EFDR < 0.1). **h)** Example violin plots showing the average log2 fold change between cells with a given gRNA and controls for select hit gRNAs. Hits include TSS positive controls (*CCND2*, *ZC3HAV1*), candidate promoters of genes rarely or not expressed NGN2, including the cortical neuron marker *TBR1*, and candidate promoters of genes with native expression in iPSC-derived neurons that could be further upregulated (*BCL11A*, *FOXP1*, and *TCF4*). Control cells are downsampled to have the same number of cells as the average number of cells detected per gRNA (n = 638) for visualization. **i)** Of 14 targeted candidate promoters, five hit gRNAs for TCF4 target the same candidate promoter that aligns with biochemical marks of regulatory activity (ATAC-Seq and H3K27ac). Empirical *P*-values are visualized alongside tracks for iPSC-derived neuron ATAC-seq (accessibility)[32], and H3K27ac[32], and RefSeq validated transcripts (ENSEMBL/NCBI). **j)** Hits included multiple gRNAs targeting *TBR1*. Genomic tracks are the same as in panel **i**.

Supplementary figures

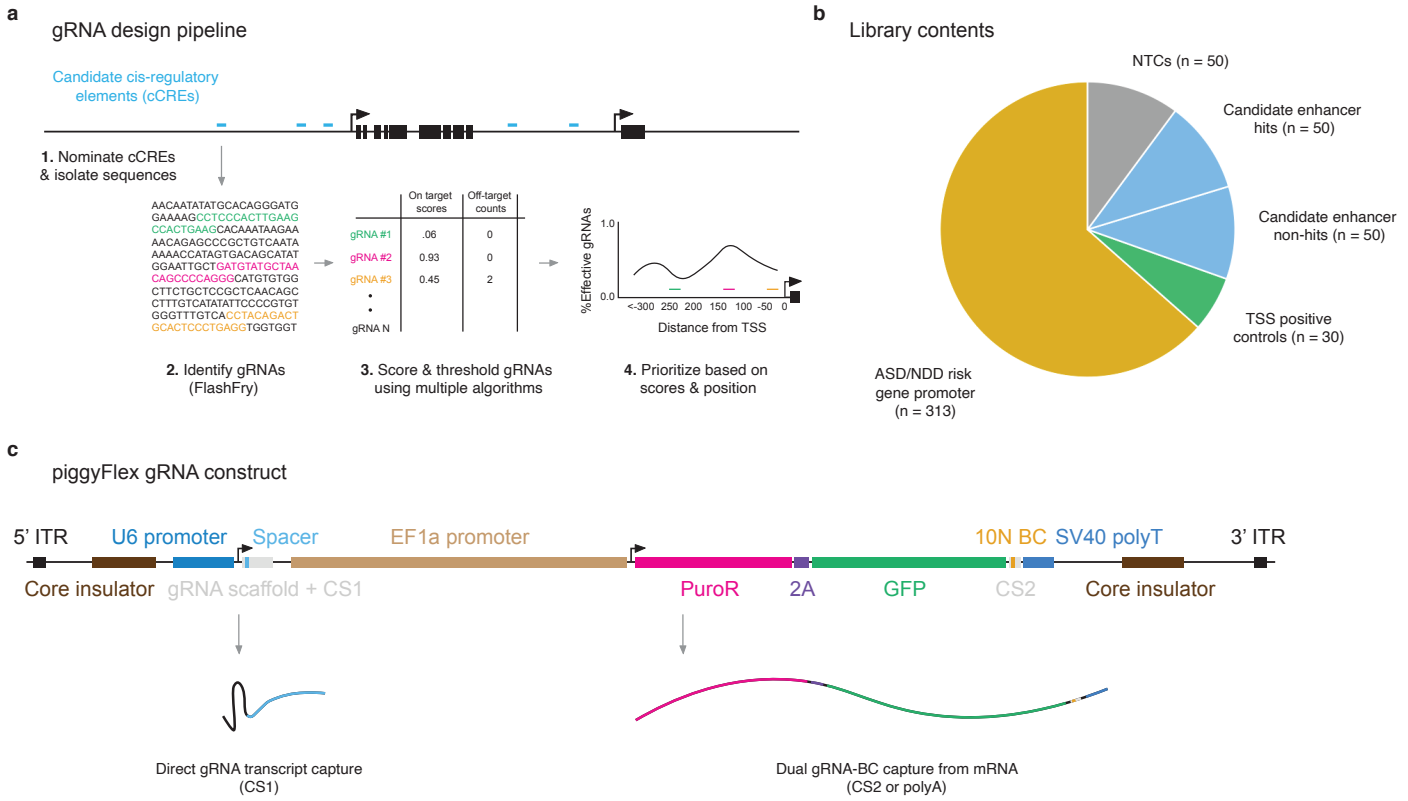

Figure S1 | gRNA design pipeline, library contents, and piggyFlex gRNA delivery construct. a) gRNA design pipeline. First, candidate Cis-Regulatory Elements (cCREs) surrounding a gene of interest were identified based on biochemical marks of regulatory activity (*e.g.*, accessibility, active transcription, etc.). Next, candidate gRNAs targeting each cCRE were generated using FlashFry[33]. Then, gRNAs were scored and prioritized using multiple algorithms. Finally, in the case of promoters where systematic CRISPRa design rules are available, gRNAs were prioritized based on optimal position relative to the TSS[28]. **b)** PiggyFlex gRNA library contents by target category. **c)** PiggyFlex construct design. PiggyFlex is a piggyBac transposon-based gRNA delivery vector equipped with a dual antibiotic (puromycin) and fluorophore (GFP) selection cassette that enables enrichment for cells with many integrated gRNAs[18]. PiggyFlex enables direct capture of gRNA transcripts or optional capture of gRNA-associated barcodes from GFP mRNA via CS2 or polydT capture.

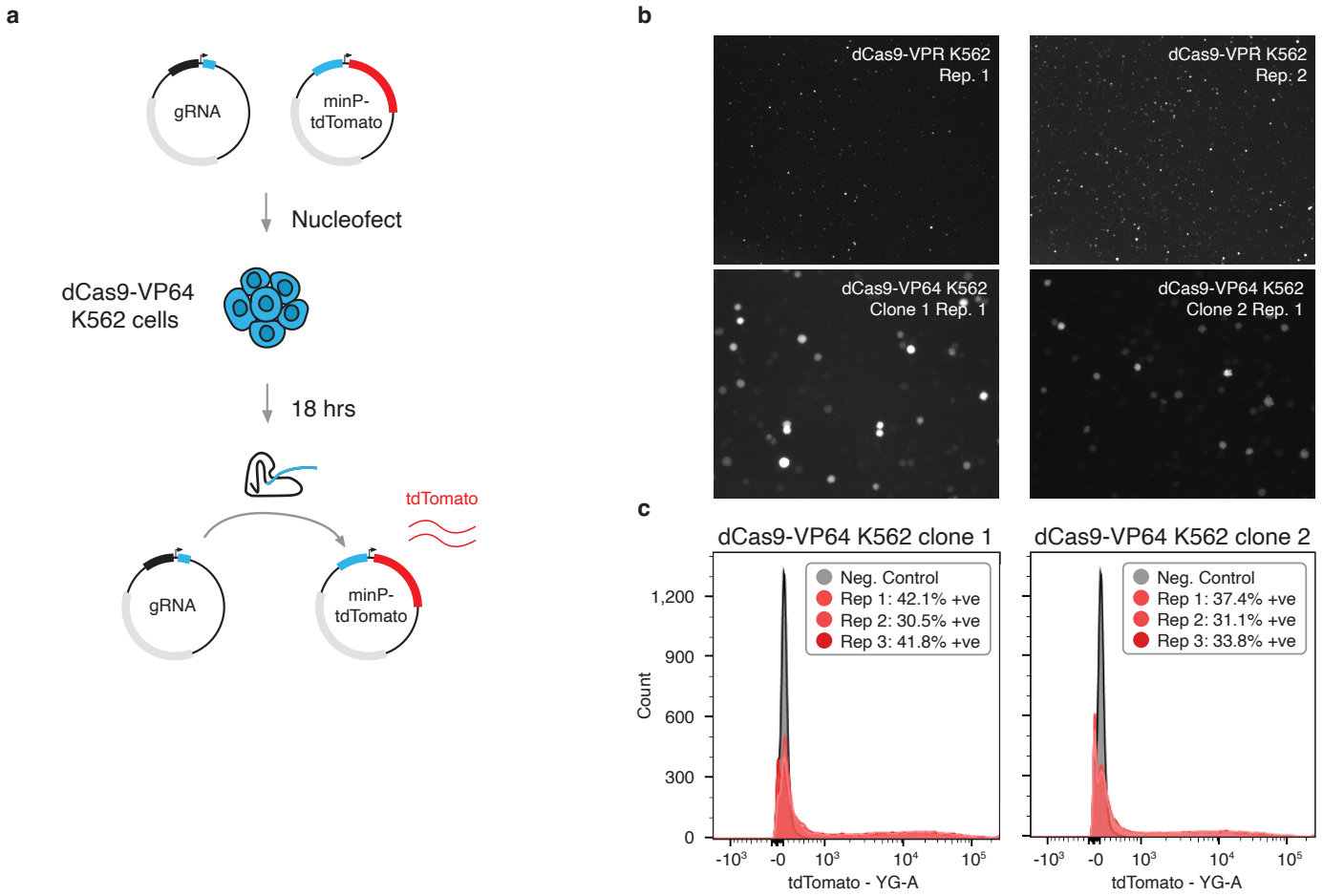

Figure S2 | Functional validation of CRISPRa K562 cell lines. a) Schematic of the minP-tdTomato functional assay used to validate CRISPRa cell lines. Two plasmids, one encoding a minP-tdTomato and another encoding a gRNA targeting a sequence immediately upstream of minP were co-nucleofected into K562 cell lines with either dCas9-VP64 or dCas9-VPR constructs integrated (only dCas9-VP64 is illustrated for simplicity). **b)** Following nucleofection, both dCas9-VPR (top, lower magnification) and dCas9-VP64 (bottom, higher magnification) K562 cell lines drove strong tdTomato expression, confirming the presence of functional CRISPRa machinery in these cell lines. dCas9-VPR images represent two replicate transfections into a single monoclonal line, while dCas9-VP64 images each represent one transfection replicate from two monoclonal lines. Note these are transient transfections without selection, so not all cells are expected to have been successfully transfected and fluoresce under these conditions. **c)** Example FACS analysis of tdTomato fluorescence in individual dCas9-VP64 transfection replicates of two monoclonal lines.

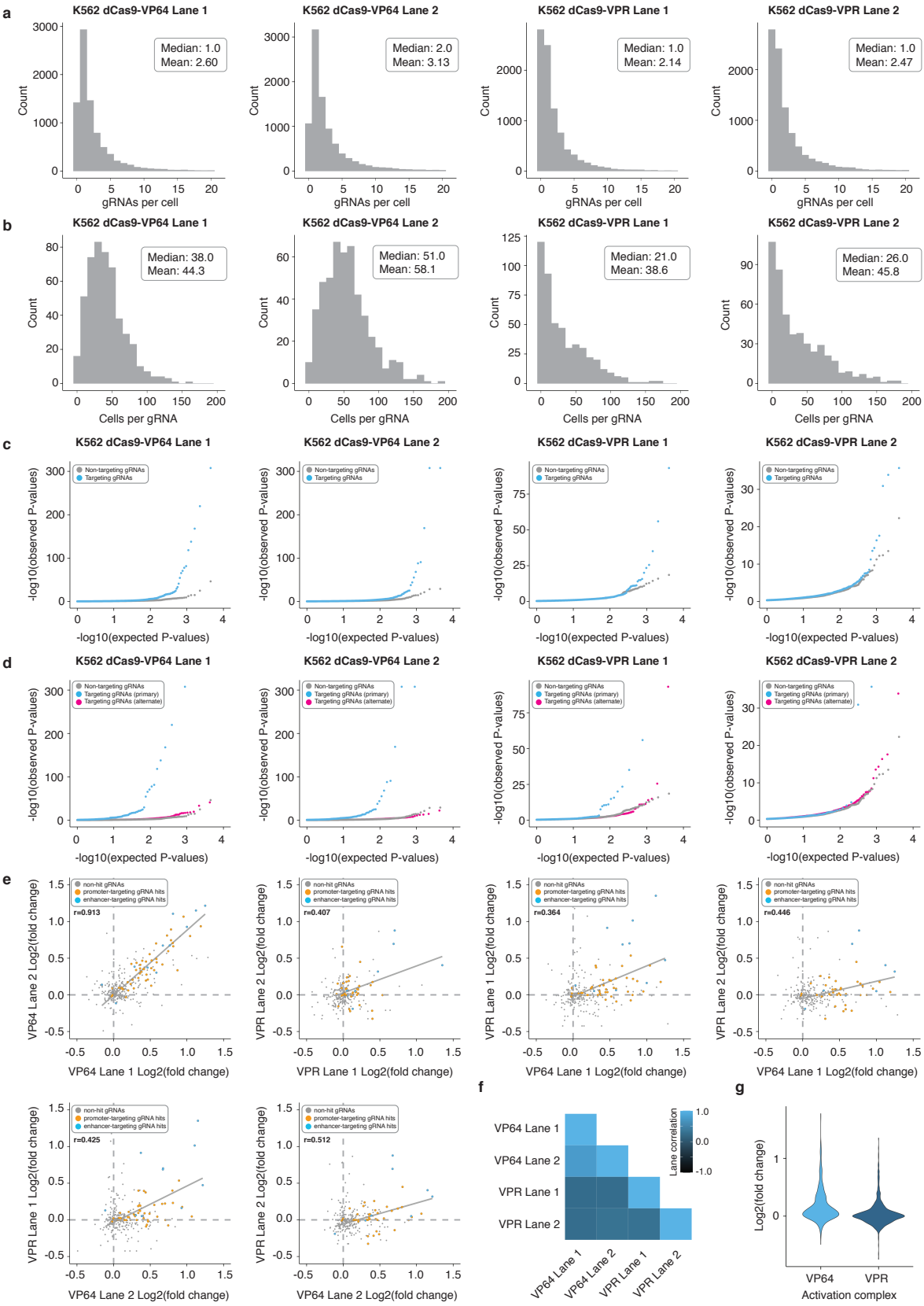

Figure S3 | Results for four independent 10x Genomics lanes from K562 screen. a) The four 10x Genomics lanes profiled included two lanes with dCas9-VP64 K562 cells and two lanes with dCas9-VPR K562 cells. Following QC and gRNA assignment we identified an average of 2.60, 3.13, 2.14, and 2.47 gRNAs/cell for the four different 10x Genomics lanes profiled (median 2.60, 3.13, 2.14, and 2.47 gRNAs per cell). PiggyBac integrations per cell distribution is not well-

modeled by a standard Poisson distribution and is better approximated by an exponential function. **b)** Multiplexing more than one perturbation per cell yielded an average of 38.0, 51.0, 21.0, and 26.0 cells/gRNA for the four different 10x Genomics lanes profiled (median 44.3, 58.1, 38.6, and 45.8 cells/gRNA). **c)** QQ-plots displaying observed vs. expected *P*-value distributions for targeting (blue) and NTC (downsampled) populations across the four different 10x Geomics lanes profiled. **d)** QQ-plots for targeting tests against their intended/programmed target (blue) compared to targeting tests of all other genes with 1Mb of each gRNA (pink) and NTCs (gray downsampled) across the four different 10x Genomics lanes profiled. **e)** Correlation plots of log2 fold changes of gRNAs across the two K562 cell lines (dCas9-VP64 and dCas9-VPR) for all four 10x Genomics lanes profiled. Pearson correlations of gRNA hits are shown. **f)** Matrix correlation plot displaying the Pearson correlations of the log2(fold change) of target gene expression values for programmed targets across the four different 10x Genomics lanes profiled. **g)** Violin plot displaying the log2(fold change) of target gene expression values for programmed targets for K562 cells harboring the dCas9-VP64 activation complex and the dCas9-VPR activation complex.

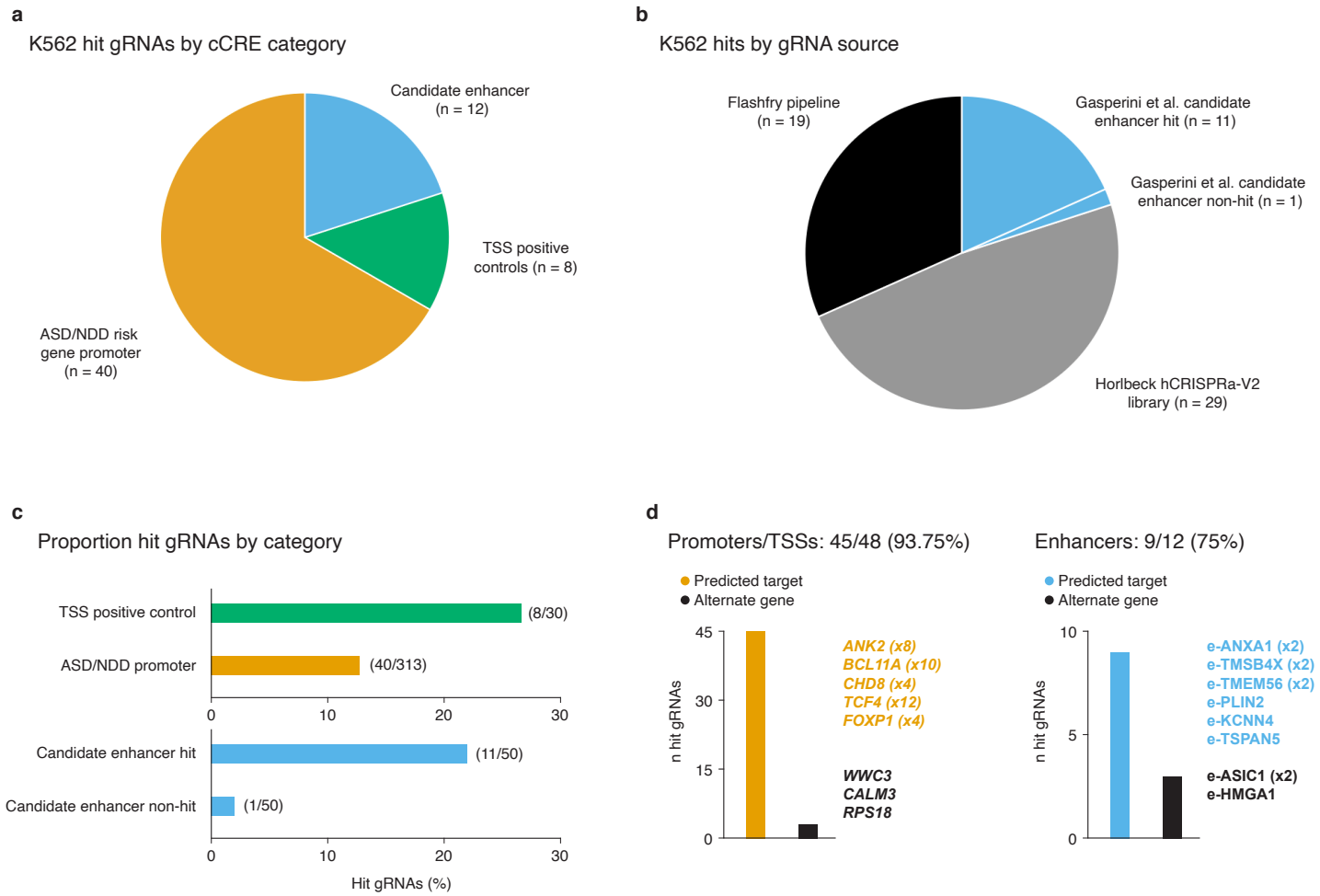

Figure S4 | Hit breakdown for screen conducted in K562 cells. a) K562 hit gRNAs by cCRE category. **b)** K562 hit gRNAs by gRNA source library or design pipeline. **c)** Proportion of hit gRNAs by cCRE category. **d)** Proportion of hit gRNAs yielding upregulation of their intended/expected target gene or an alternate gene for candidate promoters/TSSs (left) or enhancers (right). Example hits targeting candidate NDD risk gene promoters (left) and K562 enhancers (right) are listed. Bracketed numbers denote the number of independent hit gRNAs targeting the same cCRE.

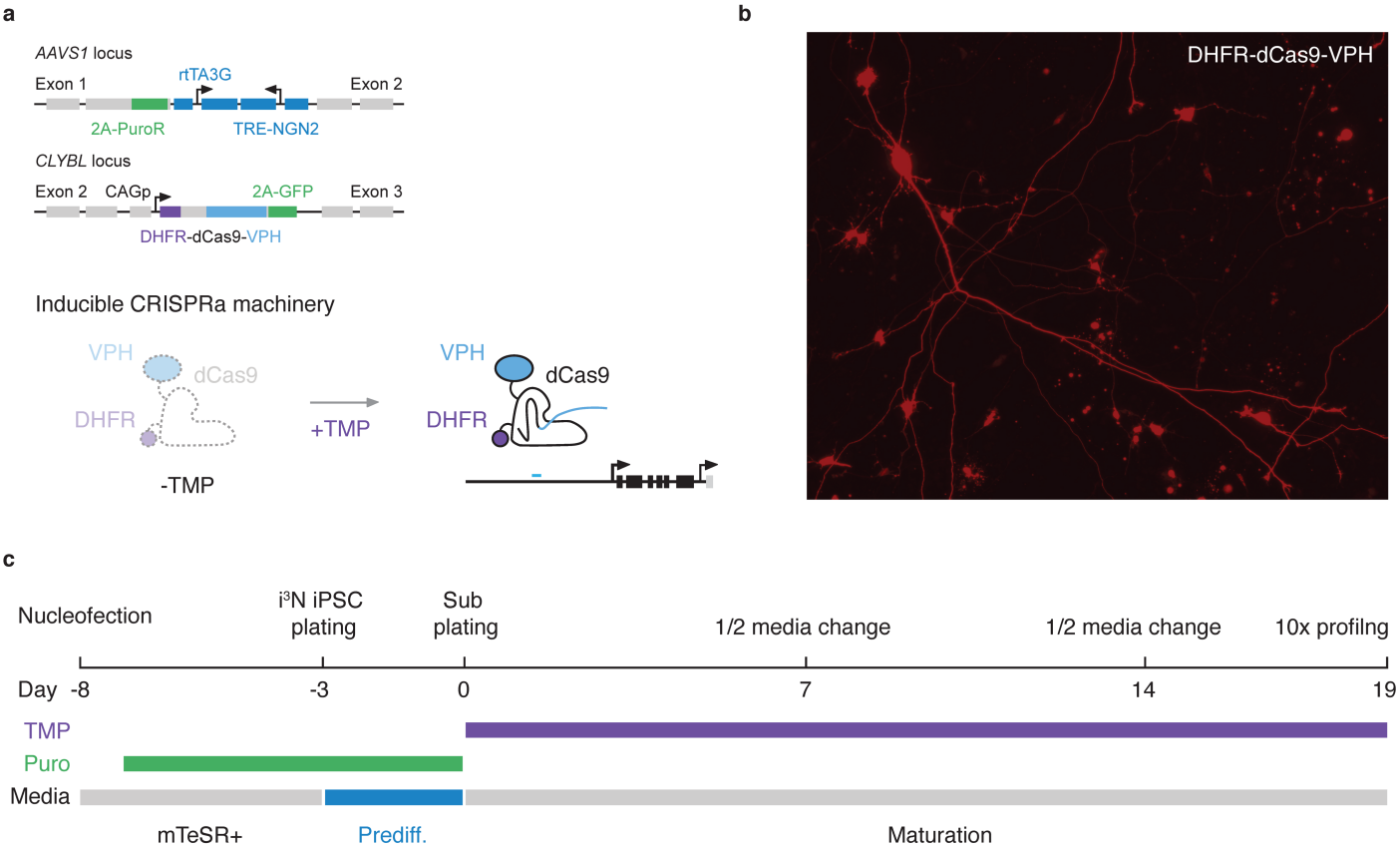

Figure S5 | Inducible CRISPRa iPSC-derived neuron line functional validation, selection, and differentiation timeline. a) (Top) iPSCs equipped with a Dox-inducible *NGN2* transcription factor to drive neural differentiation (integrated at the *AAVS1* safe harbor locus) and TMP-inducible CRISPRa-VPH machinery (integrated at the *CLYBL* locus) were used for all iPSC-derived neuron experiments. (Bottom) In the absence of TMP, CRISPRa-VPH machinery is degraded via a DHFR degron. In the presence of TMP, the CRISPR-VPH machinery is stabilized, enabling perturbation. **b)** Functional validation of CRISPRa machinery in iPSC-derived neurons. Neurons were lipofected with a minP-tdTomato reporter and sgRNA that targets the minimal promoter. CRISPRa machinery drove clear tdTomato expression in differentiated neurons. **c)** Nucleofection, selection, and differentiation timeline. iPSCs were nucleofected with piggyFlex gRNA constructs at a high MOI and selected with puromycin to enrich cells for with multiple integrated gRNAs. Following differentiation induction neurons were subplated in maturation media with TMP to induce CRISPRa machinery. Neurons were single cell profiled following 19 days of differentiation (10x Genomics V3.1 chemistry with direct gRNA capture).

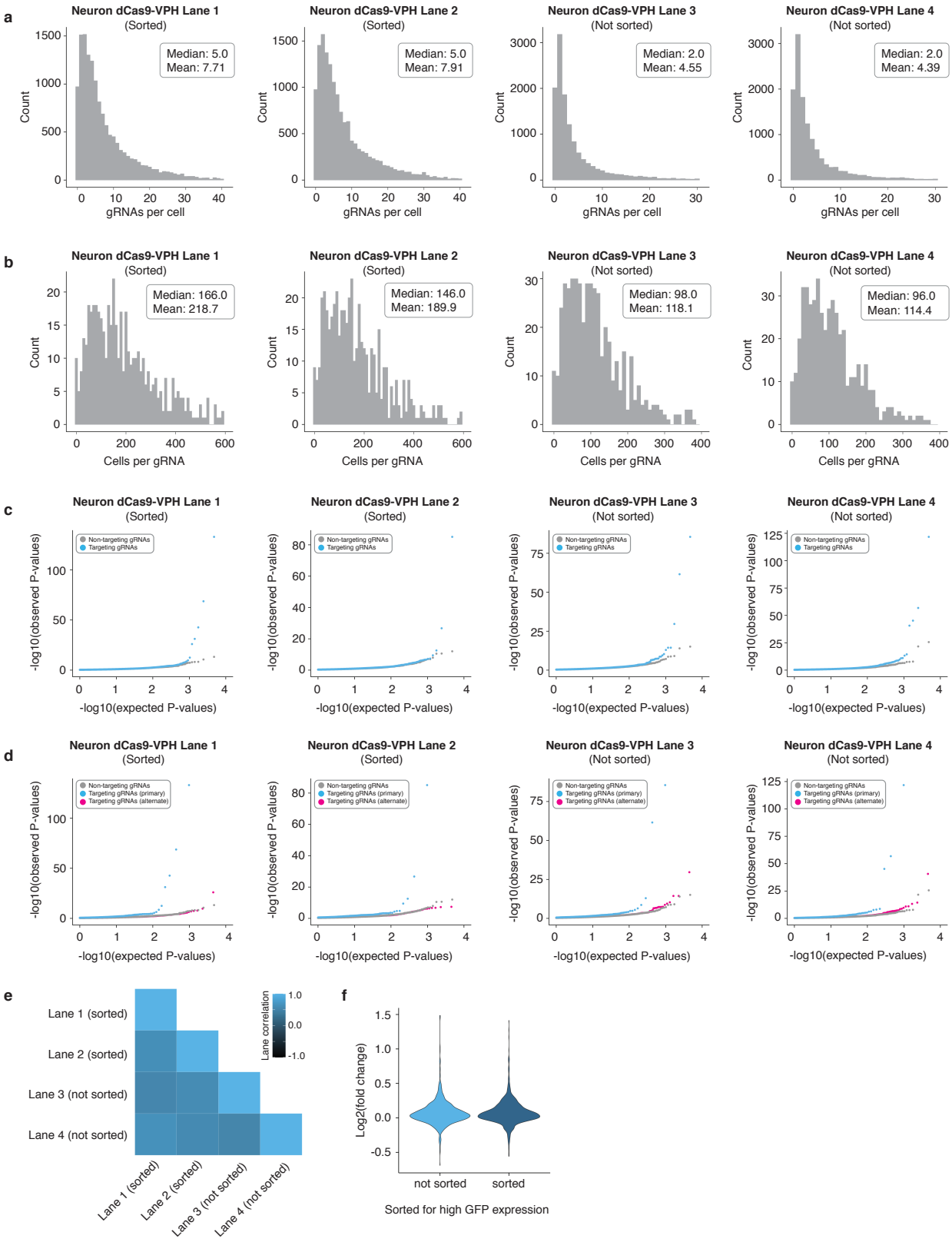

Figure S6 | Results for four independent 10x Genomics lanes from iPSC-derived neuron screen. a) The four 10x Genomics lanes profiled consisted of two lanes with dCas9-VPH neurons that were sorted on the top 40% of GFP expression in these cells, and two lanes that were not on the top 40% of GFP expression in these cells. The cells that were not sorted were still 100% GFP+. Following QC and gRNA assignment we identified an average of 7.71, 7.91, 4.55, and 4.39 gRNAs/cell for the four different 10x Genomics lanes profiled (median 7.71, 7.91, 4.55, and 4.39 gRNAs per

411 cell). Note that sorting neurons on the top 40% of GFP expression boosted the median and mean gRNAs/cell ~2 fold.
412 PiggyBac integrations per cell distribution is not well-modeled by a standard Poisson distribution and is better
413 approximated by an exponential function. **b)** Multiplexing multiple perturbations per cell yielded an average of 218.7,
414 189.9, 118.1, and 114.4 cells/gRNA for the four different 10x Genomics lanes profiled (median 166, 146, 98, and 96
415 cells/gRNA). **c)** QQ-plots displaying observed vs. expected *P*-value distributions for targeting (blue) and NTC
416 (downsampled) populations across the four different 10x Genomics lanes profiled. **d)** QQ-plots for targeting tests against
417 their intended/programmed target (blue) compared to targeting tests of all other genes with 1Mb of each gRNA (pink)
418 and NTCs (gray downsampled) across the four different 10x Genomics lanes profiled. **e)** Matrix correlation plot displaying
419 the Pearson correlations of the log2(fold change) of target gene expression values for programmed targets across the
420 four different 10x Genomics lanes profiled. **f)** Violin plot displaying the log2(fold change) of target gene expression values
421 for programmed targets for neurons that were sorted on the top 40% GFP expression (sorted) and neurons that were not
422 sorted (not sorted)

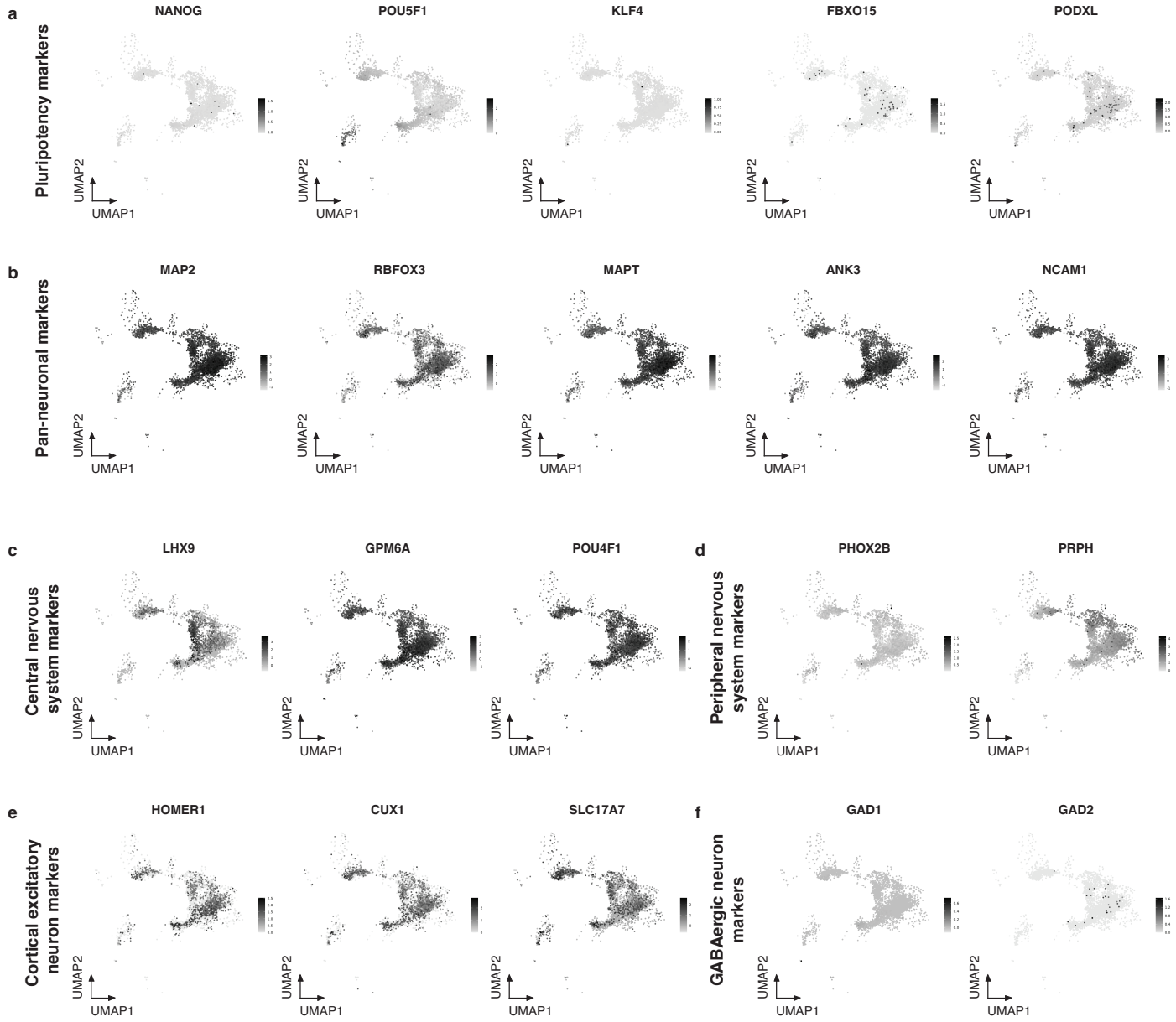

Figure S7 | Single-cell transcriptomic characterization of iPSC-derived neurons used in screen. a) Expression feature plots of canonical pluripotency markers *NANOG*, *POU5F1*, *KLF4*, *FBXO15*, and *PODXL*. **b)** Expression feature plots of pan-neuronal markers *MAP2*, *RBFOX3*, *MAPT*, *ANK3*, and *NCAM1*. **c)** Expression feature plots of central nervous system marker genes *LHX9*, *GPM6A*, and *POU4F1*. **d)** Expression feature plots of peripheral nervous system marker genes *PHOX2B* and *PRPH*. **e)** Expression feature plots of cortical excitatory neuron markers *HOMER1*, *CUX1*, and *SLC17A7*. **f)** Expression feature plots of GABAergic neuron marker genes *GAD1* and *GAD2*.

Figure S8 | Distribution of CRISPRa gRNAs in single-cell neuron transcriptome data. Cells harboring specific CRISPRa gRNAs (dark blue) overlaid onto *NGN2*-induced neuron differentiation transcriptome data[25]. No readily apparent spatial enrichment of gRNAs is observed in UMAP plots. Note that the CRISPRa dataset was randomly downsampled to 5000 cells for all UMAP comparison analyses.

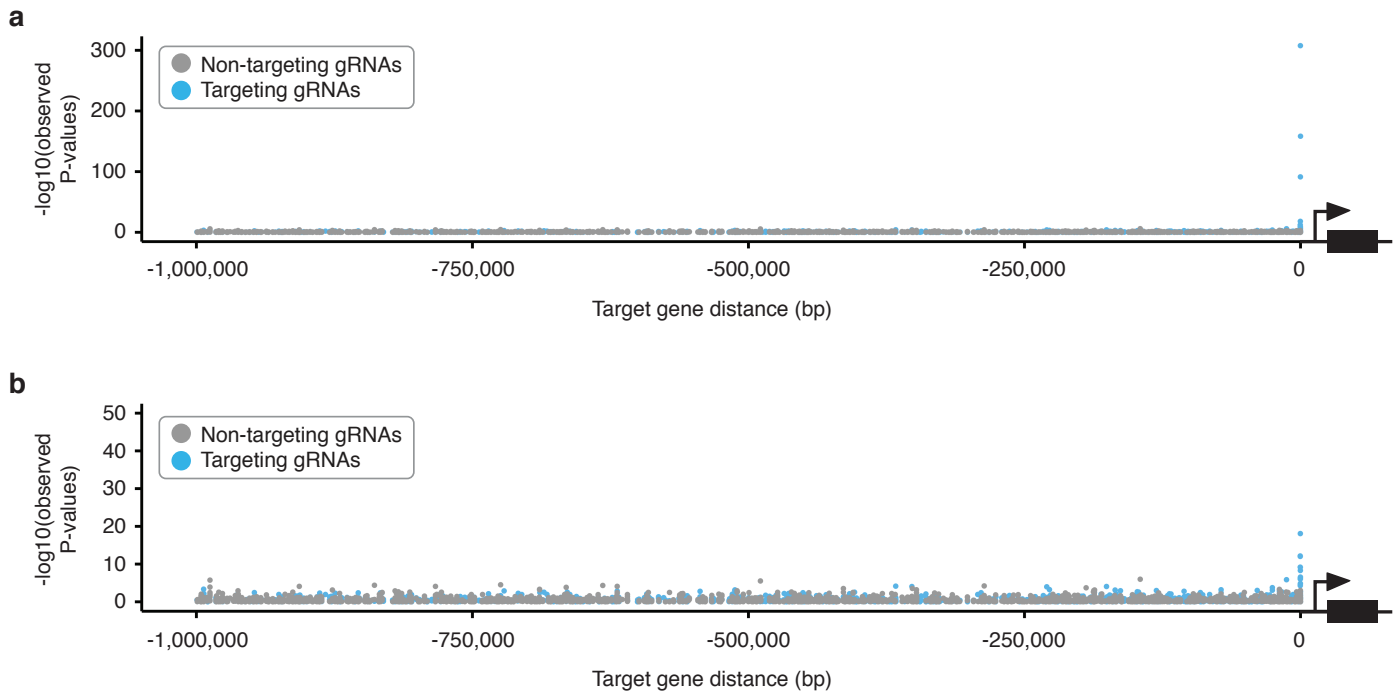

Figure S9 | Successful targeting gRNAs are enriched for genomic proximity to their paired target gene scores near target genes in the iPSC-derived neurons. a) Targeting gRNAs yielding significant upregulation are enriched for proximity to their target gene, while NTCs are not. **b)** Same plot as in **a**, with the y-axis clipped at 50.

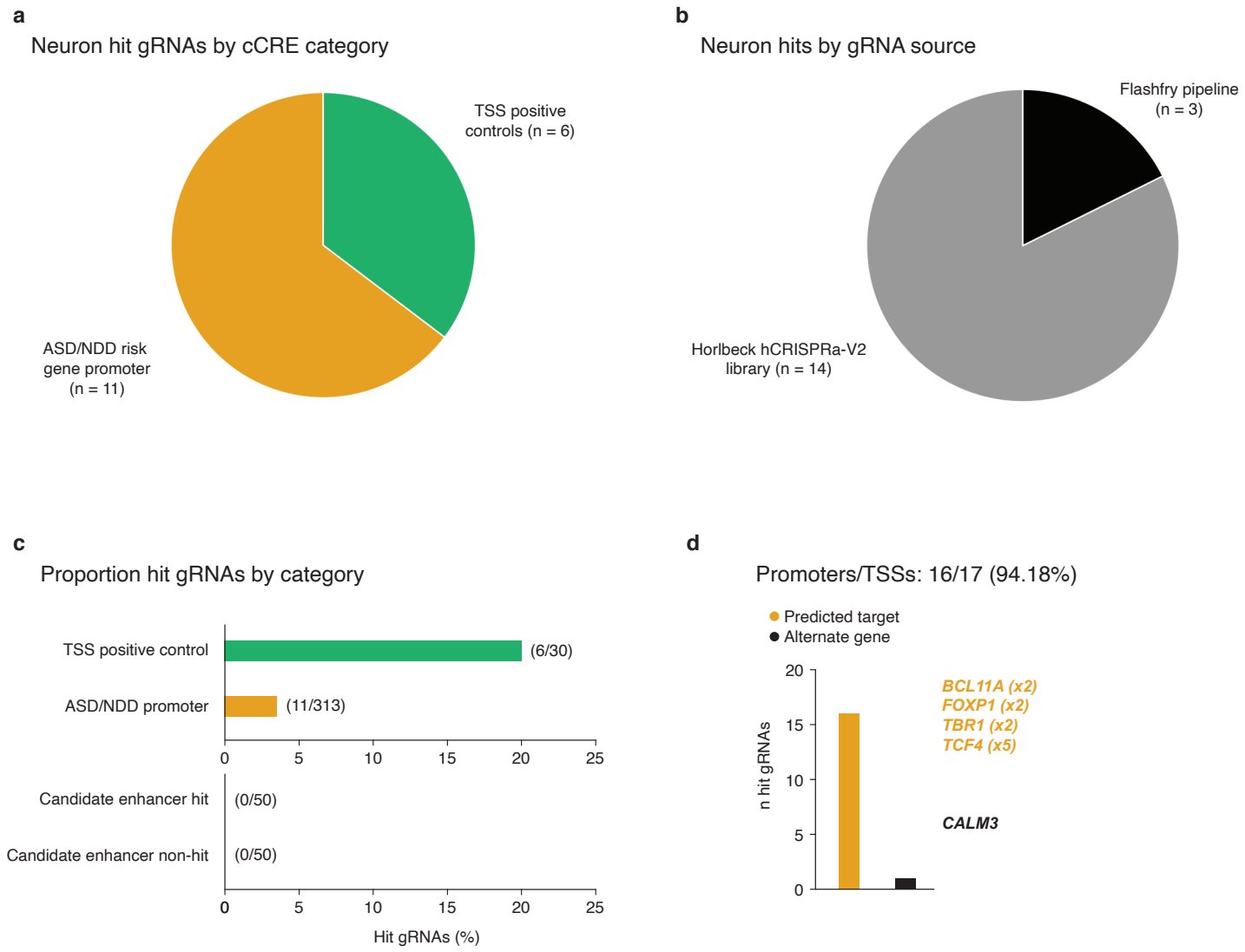

Figure S10 | Hit breakdown for screen conducted in iPSC-derived neurons. a) Neuron hit gRNAs by cCRE category. **b)** Neuron hit gRNAs by gRNA source library or design pipeline. **c)** Proportion of hit gRNAs by cCRE category. **d)** Proportion of hit gRNAs yielding upregulation of their intended/expected target gene or an alternate gene for candidate promoters/TSSs. Example hits targeting candidate NDD risk gene promoters are listed. Bracketed numbers denote the number of independent hit gRNAs targeting the same cCRE.

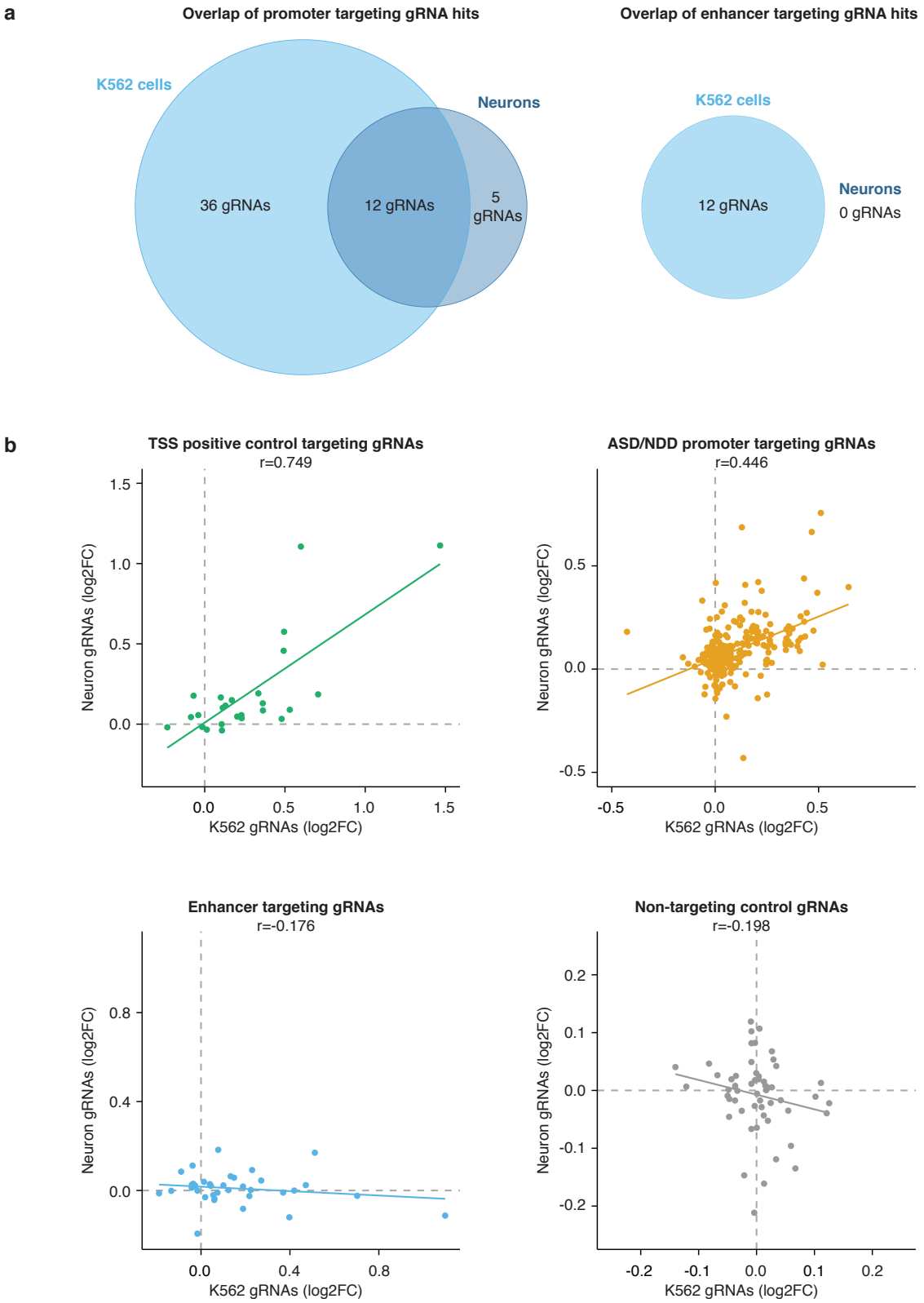

Figure S11 | Comparison of K562 vs. neuronal CRISPRa screening hits. a) Venn diagram showing number of overlapping promoter-targeting gRNA hits (left) and enhancer-targeting gRNA hits (right) between the K562 and neuron CRISPRa screens. **b)** Correlation plots of log2 fold changes of TSS positive control targeting gRNAs (top left), ASD/NDD promoter targeting gRNAs (top right), enhancer targeting gRNAs (bottom left), and NTC gRNAs (bottom right) between the K562 and neuron CRISPRa screens.

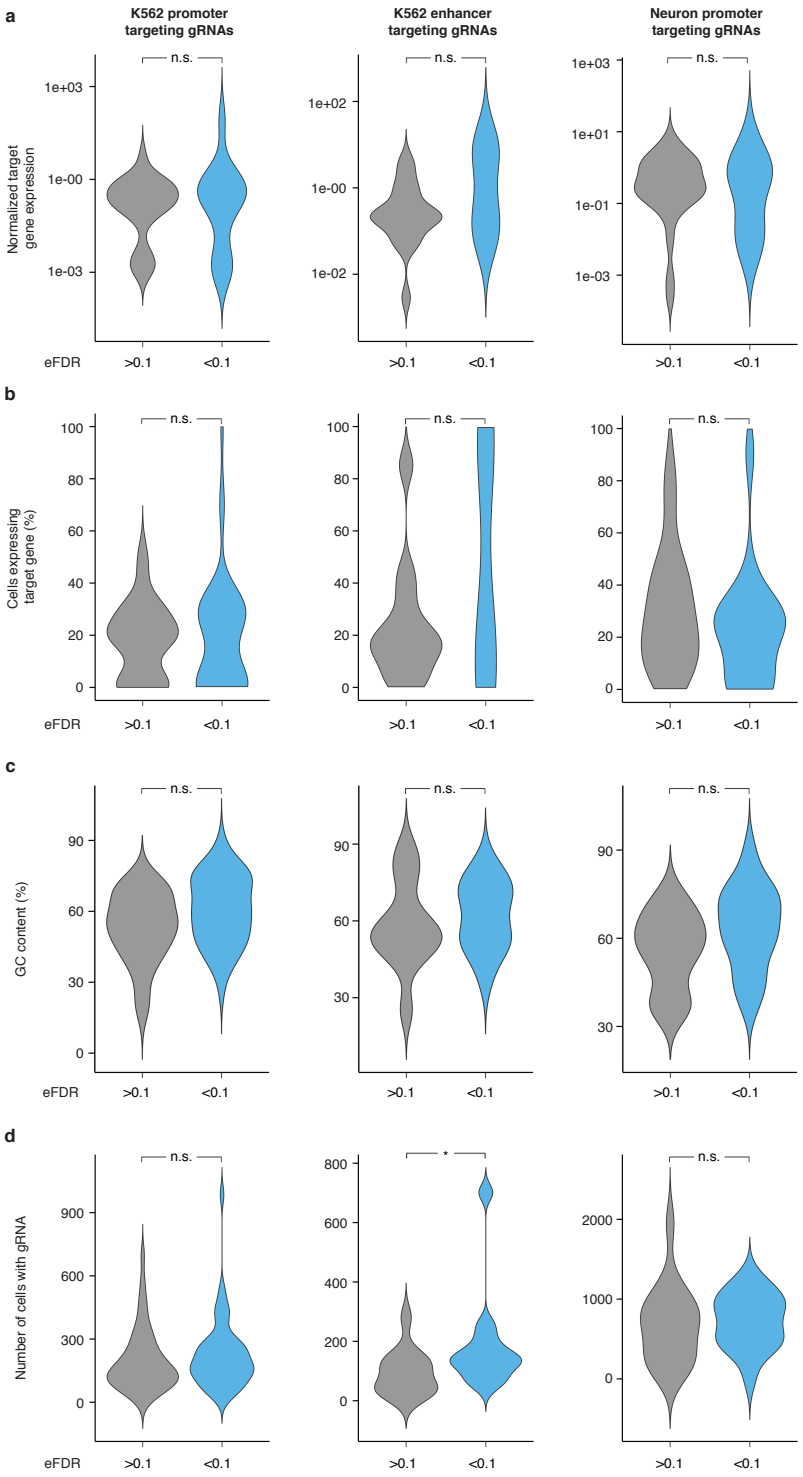

Figure S12 | Characteristics of gRNAs leading to upregulation at EFDR<0.1 vs. EFDR>0.1. a) Comparison of normalized gene expression values of targeted genes of gRNAs that resulted in an EFDR<0.1 (designated as "hit" gRNAs) versus gRNAs that resulted in an EFDR>0.1 (not designated as "hit" gRNAs). **b)** Comparison of the percentage of cells expressing the target gene of gRNAs that resulted in an EFDR<0.1 versus gRNAs that resulted in an EFDR>0.1. **c)** GC content (in percent) of gRNAs that resulted in an EFDR<0.1 versus gRNAs that resulted in an EFDR>0.1. **d)** Number of cells harboring each gRNA for gRNAs that resulted in an EFDR<0.1 versus gRNAs that resulted in an EFDR>0.1. For all panels, K562 promoter-targeting gRNAs (left), K562 enhancer-targeting gRNAs (middle), and neuron promoter-targeting gRNAs (right) are shown. Abbreviations: n.s.: not significant (p>0.05, Wilcoxon rank sum test), *: p<0.05 (Wilcoxon rank sum test).

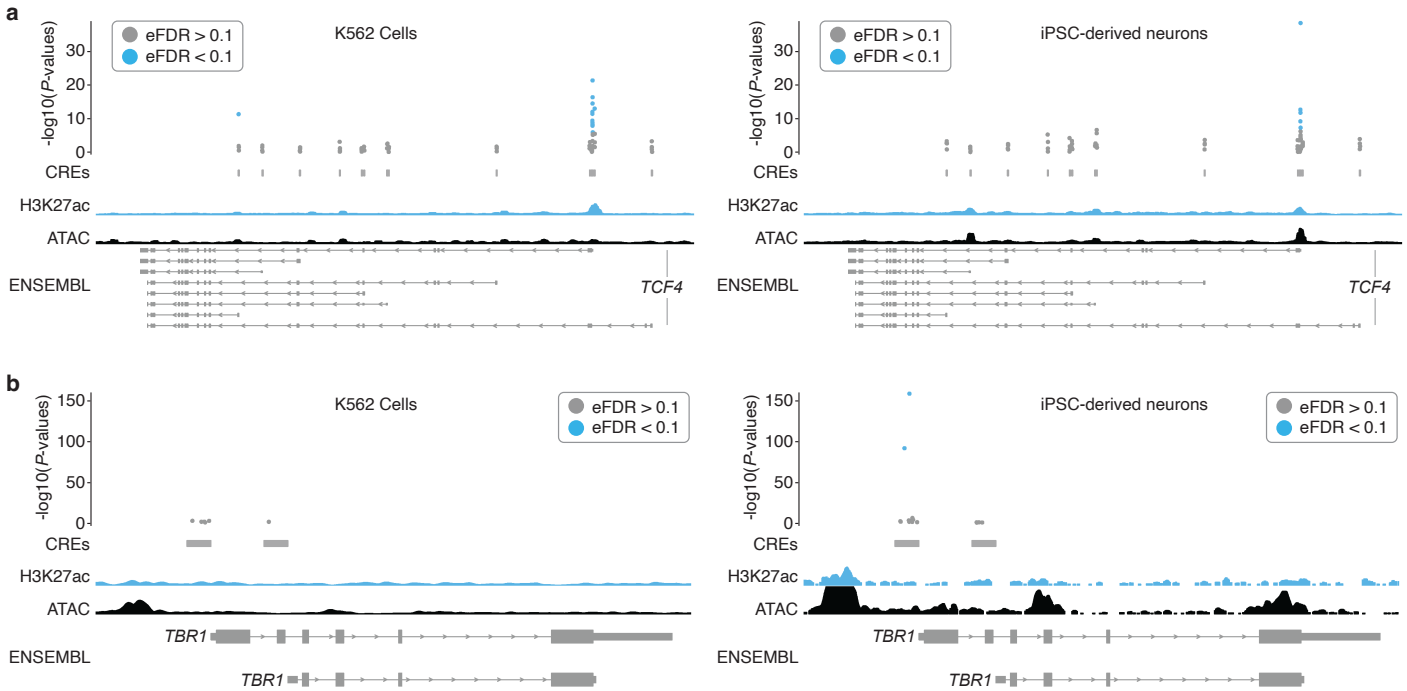

Figure S13 | TSS and cell-type specific promoters. a) The majority of hit gRNAs for *TCF4* target the same TSS in K562 cells and iPSC-derived neurons. Empirical *P*-values are visualized alongside tracks for K562 ATAC-seq (ENCODE), K562 H3K27ac signal (ENCODE), iPSC-derived neuron ATAC-seq (accessibility)[32], iPSC-derived neuron H3K27ac[32] and RefSeq validated transcripts (ENSEMBL/NCBI). **b)** Two hit gRNAs targeting the same TSS of *TBR1* drive upregulation specifically in iPSC-derived neurons. Genomic tracks are the same as in panel **a**.

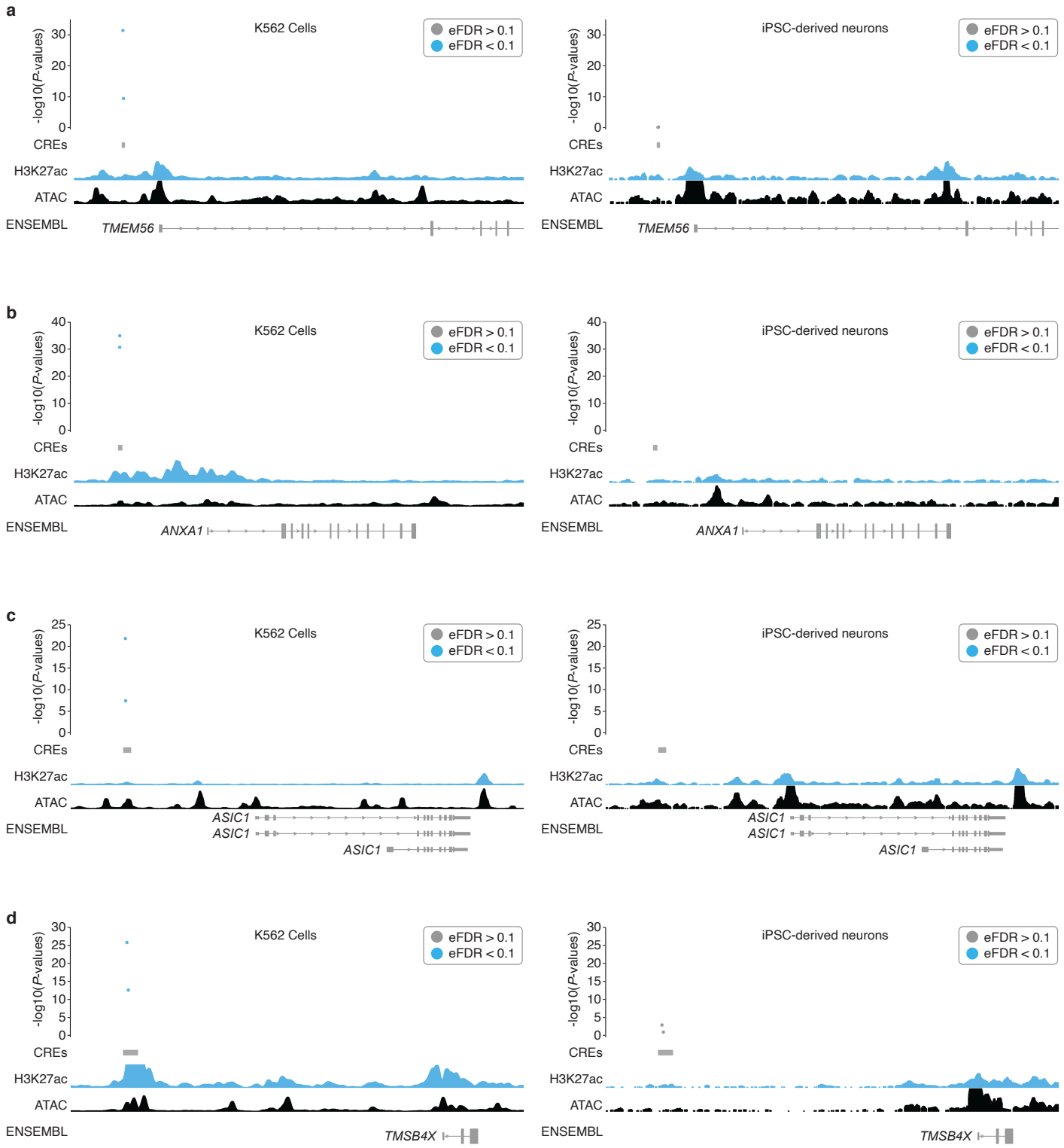

Figure S14 | Cell-type specific enhancers. a-d) Empirical *P*-values are visualized alongside tracks for K562 ATAC-seq (ENCODE), K562 H3K27ac signal (ENCODE), iPSC-derived neuron ATAC-seq (accessibility)[32], iPSC-derived neuron H3K27ac[32] and RefSeq validated transcripts (ENSEMBL/NCBI). All K562 enhancer hits were cell type specific. Enhancers with multiple hit gRNAs are shown.

Acknowledgements

We are grateful to members of the Shendure and Ahituv labs, as well as members of the Sanders, Bender, Bateup, and Feldman labs for comments, suggestions, and discussions on this work. We are particularly grateful to the Shendure lab gene regulation subgroup for technical advice and deep discussions regarding the development of the CRISPRa screening method. The Human WTC11 *NGN2* ecDHFR-dCas9-VPH line was a kind gift from the M. Kampmann lab at UCSF. Lenti dCAS9-VP64_GFP (Addgene plasmid # 61422) was a kind gift from the F. Zhang lab at Broad/MIT.

Funding

This work was supported by the Weill Neurohub (to S.J.S., N.A., and J.S.), the National Human Genome Research Institute (UM1HG011966 to N.A. and J.S.) and the National Institute of Mental Health (U01MH122681 and R01MH116999 to S.J.S.). T.A.M was supported by a Banting Postdoctoral Fellowship from the Natural Sciences and Engineering Research Council of Canada (NSERC). N.F.P. was supported by a National Science Foundation (NSF) graduate research fellowship. D.C. was supported by award no. F32HG011817 from the National Human Genome Research Institute. J.S. is an Investigator of the Howard Hughes Medical Institute.

Author contributions

Conceptualization, J.S. and N.A.; Investigation, F.M.C., T.A.M., and N.F.P.; Data Curation, F.M.C., T.A.M., and N.F.P; Formal Analysis, F.M.C., T.A.M., and N.F.P.; Visualization, F.M.C. and T.A.M.; Resources, N.A. and J.S.; Supervision, L.S., S.J.S., N.A. and J.S.; Writing – Original Draft, F.M.C., T.A.M., J.S.; Writing – Review & Editing, F.M.C., T.A.M., N.F.P., B.M., S.D., S.R., J.B.L., D.C., L.S., S.J.S., N.A, and J.S.; Funding Acquisition, S.J.S., N.A., and J.S.

Competing interests

S.J.S. receives research funding from BioMarin Pharmaceutical Incorporated. N.A. is the cofounder and on the scientific advisory board of Regel Therapeutics and receives funding from BioMarin Pharmaceutical Incorporated. J.S. is a scientific advisory board member, consultant and/or co-founder of Cajal Neuroscience, Guardant Health, Maze Therapeutics, Camp4 Therapeutics, Phase Genomics, Adaptive Biotechnologies, Scale Biosciences, Sixth Street Capital and Pacific Biosciences. All other authors declare no competing interests.

Data Availability

Raw sequencing data and processed files generated in this study will be deposited to GEO. Raw data, processed data, code, and scripts used for analyses are all publicly available and are accessible via the following website: https://krishna.gs.washington.edu/content/members/CRISPRa_QTL_website/public/.

Supplementary Materials

Figures S1-S14

1. **Figure S1** - gRNA design pipeline, library contents, and piggyFlex gRNA delivery construct.
2. **Figure S2** - Functional validation of CRISPRa K562 cell lines.
3. **Figure S3** - Results for four independent 10x Genomics lanes from K562 screen.
4. **Figure S4** - Hit breakdown for screen conducted in K562 cells.
5. **Figure S5** - Inducible CRISPRa iPSC-derived neuron line functional validation, selection, and differentiation timeline.
6. **Figure S6** - Results for four independent 10x Genomics lanes from iPSC-derived neuron screen.

7. **Figure S7** - Single-cell transcriptomic characterization of iPSC-derived neurons used in screen.
8. **Figure S8** - Distribution of CRISPRa gRNAs in single-cell neuron transcriptome data.
9. **Figure S9** - Successful targeting gRNAs are enriched for genomic proximity to their paired target gene scores near target genes in the iPSC-derived neurons.
10. **Figure S10** - Hit breakdown for screen conducted in iPSC-derived neurons.
11. **Figure S11** - Comparison of K562 vs. neuronal CRISPRa screening hits.
12. **Figure S12** - Characteristics of gRNAs leading to upregulation at EFDR<0.1 vs. EFDR>0.1.
13. **Figure S13** - TSS and cell-type specific promoters.
14. **Figure S14** - Cell-type specific enhancers.

Tables S1-S7

1. **Table S1** - gRNA sequences.
2. **Table S2** - K562 full screen results.
3. **Table S3** - K562 primary target results.
4. **Table S4** - K562 hits (EFDR < 0.1).
5. **Table S5** - iPSC-derived neuron full screen results.
6. **Table S6** - iPSC-derived neuron primary target results.
7. **Table S7** - iPSC-derived neuron hits (EFDR < 0.1).

534 # Methods

535

536 **Cell Lines and Culture**

537 **K562 cell culture**

538 K562s cells are a pseudotriploid ENCODE Tier I erythroleukemia cell line derived from a female (age 53) with chronic
539 myelogenous leukemia[15]. All K562 cells were grown at 37°C, and cultured in RPMI 1640 + L-Glutamine (GIBCO, Cat.
540 No. 11-875-093) supplemented with 10% fetal bovine serum (Rocky Mountain Biologicals, Cat No. FBS-BSC) and 1%
541 penicillin-streptomycin (GIBCO/ Thermo Fisher Scientific; Cat. No. 15140122).

542

543 **Induced pluripotent stem cell (iPSC) culture**

544 Human WTC11 iPSCs equipped with a doxycycline-inducible *NGN2* transgene expressed from the *AAVS1* safe-harbor
545 locus as well as an ecDHFR-dCas9-VPH construct (VPH consists of 12 copies of VP16, fused with a P65-HSF1 activator
546 domain) expressed from the CLYBL safe-harbor locus were a gift from the Kampmann lab[6]. These iPSCs were cultured
547 in mTeSR Plus Basal Medium (Stemcell technologies; Cat. No. 100-0276) on Greiner Cellstar plates (Sigma-Aldrich;
548 assorted Cat. Nos.) coated with Geltrex™ LDEV-Free, hESC-Qualified, Reduced Growth Factor Basement Membrane
549 Matrix (Gibco; Cat. No. A1413302) diluted 1:100 in Knockout DMEM (GIBCO/Thermo Fisher Scientific; Cat. No.
550 10829018). mTeSR Plus Basal Medium was replaced every other day. When 70–80% confluent, cells were passaged by
551 aspirating media, washing with DPBS (GIBCO/Thermo Fisher Scientific; Cat. No. 14190144), incubating with StemPro
552 Accutase Cell Dissociation Reagent (GIBCO/Thermo Fisher Scientific; Cat. No. A1110501) at 37 °C for 5 min, diluting
553 Accutase 1:1 in mTeSR Plus Basal Medium, collecting cells in conical tubes, centrifuging at 800*g* for 3 min, aspirating
554 supernatant, resuspending cell pellet in mTeSR Plus Basal Medium supplemented with 0.1% dihydrochloride ROCK
555 Inhibitor (Stemcell technologies; Cat. No. Y-27632), counting and plating onto Geltrex-coated plates at the desired
556 number.

557

558 **Human iPSC-derived neuronal cell culture, differentiation, and CRISPRa induction**

559 The iPSCs described above were used for the differentiation protocol below. On day -3, iPSCs were dissociated and
560 centrifuged as above, and pelleted cells were resuspended in Pre-Differentiation Medium containing the following:
561 Knockout DMEM/F-12 (GIBCO/Thermo Fisher Scientific; Cat. No. 12660012) as the base, 1X MEM Non-Essential Amino
562 Acids (GIBCO/Thermo Fisher Scientific; Cat. No. 11140050), 1X N-2 Supplement (GIBCO/ Thermo Fisher Scientific; Cat.
563 No. 17502048), 10 ng/mL NT-3 (PeproTech; Cat. No. 450-03), 10ng/mL BDNF (PeproTech; Cat. No. 450-02), 1 ug/mL
564 Laminin mouse protein (Thermo Fisher Scientific; Cat. No. 23017015), 10 nM ROCK inhibitor, and 2 mg/mL doxycycline
565 hyclate (Sigma-Aldrich; Cat. No. D9891) to induce expression of *NGN2*. iPSCs were counted and plated at 800K cells
566 per Geltrex-coated well of a 12-well plate in 1 mL of Pre-Differentiation Medium, for three days. At day -2 and day -1,
567 media changes were performed using pre-differentiation medium without ROCK inhibitor. On day -1, 12-well plates for
568 differentiation were coated with 15 ug/mL Poly-L-Ornithine (Sigma-Aldrich; Cat. No. P3655) in DPBS, and incubated
569 overnight at 37 degrees Celsius. On day 0, the Poly-L-Ornithine coated plates were washed three times using DPBS,
570 and the plates were air dried in a 37 degree Celsius incubator until all the DPBS evaporated. Pre-differentiated cells were
571 dissociated and centrifuged as above, and pelleted cells were resuspended in Maturation Medium containing the
572 following: 50% Neurobasal-A medium (GIBCO/Thermo Fisher Scientific; Cat. No. 10888022) and 50% DMEM/F-12
573 (GIBCO/Thermo Fisher Scientific; Cat. No. 11320033) as the base, 1X MEM Non-Essential Amino Acids, 0.5X GlutaMAX
574 Supplement (GIBCO/Thermo Fisher Scientific; Cat. No. 35050061), 0.5X N-2 Supplement, 0.5X B-27 Supplement
575 (GIBCO/Thermo Fisher Scientific; Cat. No. 17504044), 10 ng/mL NT-3, 10 ng/mL BDNF, 1 ug/mL Laminin mouse protein,
576 and 2 ug/mL doxycycline hyclate. Pre-differentiated cells were subsequently counted and plated at 400,000-450,000 cells
577 per well of a 12-well plate coated with Poly-L-Ornithine in 1 mL of Maturation medium with 20 uM trimethoprim (TMP)
578 (Sigma-Aldrich, Cat No. 92131) to activate the CRISPRa machinery in these cells (TMP stabilizes the degron-tagged
579 CRISPRa machinery). On day 7, half of the medium was removed and an equal volume of fresh Maturation medium

without doxycycline was added. On day 14, half of the medium was removed and twice that volume of fresh medium without doxycycline was added. On day 19, neurons were harvested for sc-RNA-seq.

Cell line generation and CRISPRa validation

K562 cells

K562 cells expressing dCas9-VP64 were generated in-house via lentiviral integration of a dCas9-VP64-blast construct[7] (Addgene Plasmid #61422) into K562 cells. Cells were selected with 10 ug/mL blasticidin, and polyclonal cells were single-cell sorted into 96-well plates to grow up clonal cell lines expressing dCas9-VP64. Clonal cell lines were tested for CRISPRa activity by testing the ability of a CRISPRa gRNA to activate a minP-tdTomato construct[20], and the highest tdTomato expressing cell line was used for experiments. K562 cells expressing dCas9-VPR were purchased from Horizon Discovery/Perkin Elmer (catalog ID: HD dCas9-VPR-005), and these cells were tested for CRISPRa activity using the same tdTomato expression assay described above.

iPSC-derived neurons

Human WTC11 iPSCs equipped with a doxycycline-inducible *NGN2* transgene expressed from the *AAVS1* safe-harbor locus as well as an ecDHFR-dCas9-VPH construct expressed from the CLYBL safe-harbor locus were a gift from the Kampmann lab[6]. These cells were tested for CRISPRa activity using the same tdTomato expression assay that was used to validate the K562 cell lines, which is described above.

gRNA selection and design

A complete breakdown of gRNA library contents and overview of the gRNA design pipeline is illustrated in **Figure S1**. Briefly, enhancer-targeting gRNAs were selected from our CRISPRi library[2,33]. Specifically, 50 spacer sequences (2 per candidate enhancer) were randomly selected from the list of 664 significant “hit” enhancer-gene pairs in the at-scale library. Another 50 spacer sequences targeting an additional 25 candidate enhancers (again 2 per candidate enhancer) were randomly selected from candidate enhancer non-hits (*i.e.*, gRNAs from the at-scale library targeting candidate enhancer regions with strong biochemical marks predictive of regulatory activity that did not yield significant downregulation of any neighboring genes in our previous CRISPRi study). An additional 30 TSS-positive control gRNAs were randomly sampled from the top quartile of gRNAs recommended by Horlbeck *et al*. (hCRISPRa-v2 library)[16]. 50 NTC negative control spacer sequences were also selected from the hCRISPRa-v2 library[16]. The 313 candidate promoter targeting gRNAs were either selected from the Horlbeck *et al.* library[16] or designed using FlashFry[33] (**Figure S1**). Briefly, 50 candidate promoters of 9 NDD risk genes (*TCF4*, *FOXP1*, *SCN2A*, *CHD8*, *BCL11A*, *TBR1*, *SHANK3*, *SYNGAP1*, *ANK2*)[23,24] were pulled from Basic GENCODE annotations[34] and were filtered for “type” == “transcript” and “transcript_type” == “protein coding”. Separate bed files were generated for all promoter regions defined as the 500bp upstream of each protein coding transcript. Careful attention was paid to the strand orientation of each transcript when annotating promoter regions. Bed files were sorted and merged to combine multiple promoters with >1bp overlap into a single promoter annotation. Transcript bounds provided for each merged promoter begin +1bp from the end of the promoter and end at the position corresponding to the longest transcript mapping to that promoter. NGG-protospacer within these candidate promoters were identified using FlashFry and subsequently scored using default parameters (see FlashFry manuscript and user guide for a complete description of scoring metrics/algorithms)[33]. A TSS-distance metric was then calculated for each gRNA using human fetal brain 5’ Capped Analysis of Gene Expression (CAGE) data[35,36] obtained from FANTOM (https://fantom.gsc.riken.jp/5/sstar/FF:10085-102B4; CTSS, hg38). First, the strongest FANTOM annotated TSS was identified within each +/-500 bp region up and downstream of each hg38 Gencode Basic protein coding transcript TSS. For regions with a tie between the highest scoring FANTOM TSSs, the TSS position closest to Gencode annotated TSS position was prioritized. Each candidate sgRNA from FlashFry was annotated with the distance to the nearest FANTOM TSS using the command “bedtools closest -a sgRNAs_with_fantom_tss -b strongest_fantom_tss_within_gencode_promoter -D b -t first.” For Gencode Basic protein coding transcripts without a human fetal brain FANTOM peak within 500 +/- bp, the distance of each sgRNA to the nearest Gencode TSS was

627 reported instead. A distance of zero indicates that an sgRNA overlaps with the nearest annotated TSS. Multiple rounds
628 of successively relaxing score and distance thresholds were then iterated until the top 4 gRNAs for each candidate
629 promoter were selected (five selection rounds in total). Optimal TSS-distances were approximated using genome-wide
630 CRISPRa design rules[28]. gRNAs flagged for potentially problematic polythymidine tracks or GC content were excluded.
631 The gRNA selection criteria used in each round were as follows:

632 **Round 1: 1.** TSS Distance between -150 and -75 BP **2.** Doench2014OnTarget >= 0.2 **3.** Dangerous_in_genome
633 <= 1 **4.** Hsu2013 > 80.

634 **Round 2: 1.** TSS Distance between -400 and -50 BP **2.** Doench2014OnTarget >= 0.2 **3.** Dangerous_in_genome
635 <= 1 **4.** Hsu2013 > 80.

636 **Round 3: 1.** TSS Distance between -400 and -50 BP **2.** Doench2014OnTarget >= 0.2 **3.** Dangerous_in_genome
637 <= 1 **4.** Hsu2013 > 50.

638 **Round 4: 1.** TSS Distance between -400 and -50 BP 2. Doench2014OnTarget >= 0.2 3. Dangerous_in_genome
639 <= 2 4. Hsu2013 > 50.

640 **Round 5: 1.** Doench2014OnTarget >= 0.2 **2.** Dangerous_in_genome <= 2 **3.** Hsu2013 > 10 **4.**
641 DoenchCFD_maxOT < 0.95

642

643 Complete oligo sequences with gRNA spacers and additional sequences for cloning into piggyFlex are listed in **Table**
644 **S1**. Note all gRNAs in our library are designed/modified to start with a G followed by the 19 base pair spacer to facilitate
645 Pol III transcription.

646

647 **gRNA library cloning into piggyFlex vector**

648 The 493 gRNAs with associated 10N random barcodes were ordered as an IDT oPool and PCR amplified with Q5 High-
649 Fidelity polymerase (NEB, Cat. No. M0491S) to make double stranded DNA. The piggyFlex backbone vector was
650 digested with SalI (NEB, Cat. No. R3138S) and BbsI (NEB, Cat. No. R0539S) in 10X NEBuffer r2 at 37 degrees Celsius
651 overnight to ensure complete digestion of the backbone. This digestion cuts out the EF1a-puro-GFP cassette of the
652 vector which is then added back in a later cloning step. The digestion product was run on a 1% agarose gel in TAE buffer,
653 and the linear backbone vector (5098 base pairs in size) was gel extracted using a gel extraction kit (NEB, Cat. No.
654 T1020S). The second product from the digestion (2878 base pairs) which contains the EF1a-puro-GFP cassette was
655 saved for a later assembly reaction in the final cloning step (described below). The PCR amplified IDT oPool gRNAs with
656 associated 10N random barcodes were cloned into the linear backbone using NEBuilder HiFi DNA Assembly (NEB, Cat.
657 No. E2621S) using 0.15 pmol of the insert (gRNA library) and 0.02 pmol of the linear backbone. Assembled product was
658 transformed into electrocompetent cells (NEB, Cat. No. C3020K) and plasmid DNA was extracted with a midiprep kit
659 (Zymo Research, Cat. No. D4200). The resulting vector was then digested with SapI (NEB, Cat. No. R0569S), for one
660 hour at 37 degrees Celsius. Digested product was cleaned with 0.5X AMPure beads (Beckman Coulter, Cat. No. A63880)
661 and cleaned digested linear backbone was used for a subsequent assembly reaction to add the EF1a-puro-GFP
662 cassette back into the final piggyFlex vector between the gRNA sequence and the 10N random barcode sequences.
663 0.014 pmol of the linear backbone was assembled with 0.056 pmol of the insert sequence and the assembly
664 reaction was cleaned with a 0.5X AMPure step. The assembled product was transformed into electrocompetent cells
665 and plasmid DNA was extracted with a midiprep kit. The final plasmid library was subsequently PCR amplified and
666 sequenced to ensure that all 493 gRNAs were successfully cloned into the piggyFlex vector. Note: The 10N barcode is
667 an additional gRNA identification strategy that can be used to assign gRNAs to cells, however, we used directly
668 sequenced gRNAs (from the 10x Genomics capture sequence) to identify gRNAs in this work as this more accurately
669 assigns gRNA transcripts to cells[37].

670

671 **Transfection of the gRNA library and selection for transfected cells**

672 **K562 cells**

673 16 million K562 cells (8 million K562-VP64 cells and 8 million K562-VPR cells) were transfected with the gRNA library
674 and the piggyBac transposase (System Biosciences, Cat. No. PB210PA-1) at a 20:1 molar ratio of library:transposase
675 using a Lonza 4D nucleofector and the Lonza nucleofector protocol for K562 cells. The 16 million cells were split across
676 8 100 uL nucleofection cartridges, with each individual nucleofection cartridge receiving 2 million cells and 2 ug of total
677 DNA. After nucleofection, cells were transferred to pre-warmed RPMI media in a cell culture flask and incubated at 37
678 degrees Celsius. One day after transfection, cells were selected with 2 ug/mL puromycin (GIBCO/Thermo Fisher
679 Scientific; Cat. No. A1113803). After 9 days, cells were harvested for single-cell transcriptome profiling.

680

681 **Induced pluripotent stem cells**

682 6 million dCas9-VPH iPSCs (same cells as described above) were transfected with the gRNA library and the piggyBac
683 transposase at a 5:1 molar ratio of library:transposase using the Lonza nucleofector and the Lonza nucleofector CB-150
684 program. The 6 million cells were split across 6 100 uL nucleofection cartridges, with each individual nucleofection
685 cartridge receiving 1 million cells and 17.5 ug of total DNA. After nucleofection, cells were transferred to pre-warmed
686 mTeSr Plus basal medium with ROCK inhibitor in a cell culture flask and incubated at 37 degrees Celsius. One day after
687 transfection, cells were selected with 20 ug/mL puromycin (note: the AAVS1-NGN2 construct has a puromycin resistance
688 cassette on it, so a higher dose of puromycin was used to successfully select for cells that received a gRNA in the
689 presence of an existing puromycin resistance cassette). Media changes were performed daily (mTeSr Plus basal medium
690 with ROCK inhibitor and 10 ug/mL puromycin) for seven days prior to initiating neuron differentiation (described in "Human
691 iPSC-derived neuron cell culture and differentiation" methods section).

692

693 **<u>10x Genomics sc-RNA-seq with associated gRNA transcript capture</u>**

694 **K562 screen**

695 Cells were harvested and prepared into single-cell suspensions following the 10x Genomics Single Cell Protocols Cell
696 Preparation Guide (Manual part number CG00053, Rev C). Four lanes were used for the single-cell transcriptome
697 profiling, with two lanes containing cells from the K562-VP64 cell line, and two lanes containing cells from the K562-VPR
698 cell line. Roughly 10,000 cells were captured per lane of a 10x Chromium chip (Next GEM Chip G) using Chromium Next
699 GEM Single Cell 3' Reagent Kits v3.1 with Feature Barcoding technology for CRISPR Screening (10x Genomics, Inc,
700 Document number CG000205, Rev D).

701

702 **iPSC-derived neuron screen**

703 iPSC-derived neurons were harvested and prepared into single-cell suspensions following a published protocol [38]. Cells
704 were split into two batches, with one batch going through a fluorescence-activated cell sorting (FACS) step to sort on the
705 top 40% of green fluorescent protein (GFP) expression to enrich for neurons with greater numbers of gRNAs integrated,
706 and the second batch going directly into the 10x Genomics single-cell library preparation protocol. Sorting on the top 40%
707 of GFP expression resulted in a two-fold increase in the mean number of gRNAs integrated in those cells as compared
708 to unsorted cells. Four lanes were used for the single-cell transcriptome profiling, with two lanes containing GFP-positive
709 sorted cells, and two lanes containing unsorted cells. Roughly 13,000 cells were captured per lane of a 10x Chromium
710 high-throughput chip (Next GEM Chip M) using Chromium Next GEM Single Cell 3' HT Reagent Kits v3.1 (Dual Index)
711 with Feature Barcode technology for CRISPR Screening (10x Genomics, Inc, Document number CG000418, Rev C).

712

713 **Sequencing of scRNA-seq libraries**

714 Final libraries were sequenced on a NextSeq 2000 P3 100 cycle kit (R1:28 I1:10, I2:10, R2:90) for each screen (K562
715 and iPSC-derived neuron screens). Gene expression and gRNA transcript libraries were pooled at a 4:1 ratio for
716 sequencing.

717

718 **Transcriptome data processing and quality control filtering for K562 and iPSC-derived neuron screens**

719 CellRanger version 6.0.1 was used to perform bcl2fastq and count matrix generation. CellRanger mkfastq was run using
720 default parameters, and CellRanger count was run using the GRCh38-3.0.0 reference transcriptome from 10x Genomics
721 and default parameters. For the K562 screen, cells with greater than 10% mitochondrial reads and less than 4000 UMIs
722 were filtered out. For the iPSC-derived neuron screen, cells with greater than 17% mitochondrial reads and less than
723 1500 unique molecular identifiers (UMIs) were filtered out. After quality control filtering, 33,944 cells were retained in the
724 K562 screen, and 51,183 cells were retained in the iPSC-derived neuron screen. The resulting count matrix output after
725 this filtering was used for all downstream analyses.

726

727 **Neuron differentiation transcriptome projection**

728 Single-cell transcriptome data from a time course study of iPSC-derived neurons[26] was downloaded from
729 https://www.ebi.ac.uk/biostudies/arrayexpress/studies/E-MTAB-10632 (Accession No. E-MTAB-10632,
730 matrices_timecourse.tar.gz), and integrated with the neuron CRISPRa screening dataset described here. Seurat v4 was
731 used for all data analyses[39]. The CRISPRa dataset was randomly downsampled to 5,000 cells for this analysis. Count
732 matrices from both matrices were filtered to include only shared genes from the two datasets (n=14,777 genes).
733 SelectIntegrationFeatures() and FindIntegrationAnchors() were run using default parameters to identify anchors for
734 integration. 20,606 anchors were found and 2,953 anchors were retained for data integration. IntegrateData() was run
735 using the retained 2,953 anchors to integrate the two datasets. After integration, standard Seurat single-cell analysis was
736 performed to scale the data, and run the PCA and UMAP algorithms.

737

738 **<u>gRNA assignment and differential gene expression testing</u>**

739 Genomic coordinates (hg38) for final gRNA spacers were isolated using a loop built around the matchPattern() function
740 from the BSgenome package[40]. A 2Mb window (1Mb upstream and downstream) around each gRNA was then calculated
741 and all genes within the 2Mb window were isolated using a loop built around ENSEMBL biomaRt getBM() function[41,42].
742 These 1Mb neighboring gene sets were then filtered to unique entries (unique HGNC symbols) for compatibility with the
743 Seurat FindMarkers() function used in DE testing.

744 A global UMI filter of 5 gRNA UMIs/cell was used to assign gRNAs to single cell transcriptomes for both K562 and iPSC-
745 derived neuron datasets (note this heuristic threshold was chosen based on manual inspection of the UMI count
746 distributions for each gRNA and prior work)[2]. gRNA UMI counts for each cell were derived from the count matrix of
747 passing cells output by CellRanger (which applies an automatic total UMI threshold to cells) and which also passed QC.

748 Expression of a given gene within 1Mb of the gRNA of interest was compared between all cells with a given gRNA and
749 all other cells as control. log2() fold changes in expression for a given gene were calculated using the Seurat
750 FindMarkers() function with the following arguments: ident.1 = gRNA_Cells, ident.2 = Control_Cells, min.pct = 0,
751 min.cells.feature = 0, min.cells.group = 0, features = target_gene, logfc.threshold = 0. A Wilcoxon rank-sum test was
752 used to generate raw differential expression *P*-values. This process was then iterated for all genes within 1Mb of all
753 gRNAs. NTCs were tested against all genes within 1Mb of any targeting gRNA. Only tests involving genes detected in
754 >0.2% of test gRNA and control cells were carried forward.

755 These raw differential expression *P*-values were then used to calculate empirical P-values to call EFDR < 0.1 sets[2].
756 Specifically, an empirical *P*-value was calculated for each gRNA-gene test as:

757

758 *[(the number of NTCs with a P-value lower than that test's raw P-value) + 1] /*

759 *[the total number of NTCs tests + 1]*

760

761 Empirical *P*-values were then Benjamini-Hochberg corrected, and those < 0.1 were kept for 10% EFDR sets.

762

763 Log2 fold changes between gRNA and control cells were visualized using the gviz package[43] along with tracks for RefSeq
764 transcripts (ENSEMBL biomaRt), H3K27ac, and ATAC seq peaks. The K562 ATAC and H3K27ac data were downloaded
765 from ENCODE [44]. ATAC-seq and H3K27ac CUT&RUN data from 7-8 week old NGN2-iPSC inducible excitatory neurons
766 was obtained from Song et al. 2019[32]. As previously described, ATAC-seq and CUT&RUN reads were trimmed to 50bp
767 using TrimGalore with the command --hardtrim5 50 before alignment (https://github.com/FelixKrueger/TrimGalore).
768 ATAC-seq reads were realigned to hg38 using the standard Encode Consortium ATAC-seq and ChIP-seq pipelines
769 respectively with default settings and pseudo replicate generation turned off. Trimmed, sorted, duplicate and chrM
770 removed ATAC-seq bam files from multiple biological replicates were combined into a single bam file using samtools
771 merge v1.10[45]. Trimmed CUT&RUN reads were realigned to hg38 using Bowtie2 v2.3.5.1 with the following settings --
772 local --very-sensitive-local --no-mixed --no-discordant -I 10 -X 700 and output sam files were convert to bam format using
773 samtools view[45,46]. Duplicated reads were removed from the CUT&RUN bam file using Picard MarkDuplicates v2.26.0
774 with the --REMOVE_DUPLICATES =true and --ASSUME_SORTED=true options (http://broadinstitute.github.io/picard/).
775 Finally, bam files were converted using the bedtools genomecov followed by the UCSC bedGraphToBigWig utility.

776 **References**

777 1. Gasperini, M., Tome, J. M. & Shendure, J. Towards a comprehensive catalogue of validated and target-linked
778 human enhancers. *Nat. Rev. Genet.* **21**, 292–310 (2020).
779 2. Gasperini, M. *et al.* A Genome-wide Framework for Mapping Gene Regulation via Cellular Genetic Screens. *Cell*
780 **176**, 377–390.e19 (2019).
781 3. Fulco, C. P. *et al.* Systematic mapping of functional enhancer–promoter connections with CRISPR interference.
782 *Science* **354**, 769–773 (2016).
783 4. Xie, S., Duan, J., Li, B., Zhou, P. & Hon, G. C. Multiplexed Engineering and Analysis of Combinatorial Enhancer
784 Activity in Single Cells. *Mol. Cell* **66**, 285–299.e5 (2017).
785 5. Gilbert, L. A. *et al.* Genome-Scale CRISPR-Mediated Control of Gene Repression and Activation. *Cell* **159**, 647–
786 661 (2014).
787 6. Tian, R. *et al.* Genome-wide CRISPRi/a screens in human neurons link lysosomal failure to ferroptosis. *Nat.*
788 *Neurosci.* **24**, 1020–1034 (2021).
789 7. Konermann, S. *et al.* Genome-scale transcriptional activation by an engineered CRISPR-Cas9 complex. *Nature*
790 **517**, 583–588 (2014).
791 8. Schmidt, R. *et al.* CRISPR activation and interference screens decode stimulation responses in primary human T
792 cells. *Science* **375**, eabj4008 (2022).
793 9. Simeonov, D. R. *et al.* Discovery of stimulation-responsive immune enhancers with CRISPR activation. *Nature*
794 **549**, 111–115 (2017).
795 10. Matharu, N. *et al.* CRISPR-mediated activation of a promoter or enhancer rescues obesity caused by
796 haploinsufficiency. *Science* **363**, (2019).
797 11. Tamura, S. *et al.* CRISPR activation rescues abnormalities in SCN2A haploinsufficiency-associated autism
798 spectrum disorder. *bioRxiv* 2022.03.30.486483 (2022) doi:10.1101/2022.03.30.486483.
799 12. Dai, Z. *et al.* Inducible CRISPRa screen identifies putative enhancers. *J. Genet. Genomics* **48**, 917–927 (2021).
800 13. Tak, Y. E. *et al.* Augmenting and directing long-range CRISPR-mediated activation in human cells. *Nat. Methods*
801 **18**, 1075–1081 (2021).
802 14. Joung, J. *et al.* Genome-scale activation screen identifies a lncRNA locus regulating a gene neighbourhood.
803 *Nature* **548**, 343–346 (2017).
804 15. Zhou, B. *et al.* Comprehensive, integrated, and phased whole-genome analysis of the primary ENCODE cell line
805 K562. *Genome Res.* **29**, 472–484 (2019).

806 16. Horlbeck, M. A. *et al.* Compact and highly active next-generation libraries for CRISPR-mediated gene repression
807 and activation. *Elife* **5**, (2016).
808 17. Matharu, N. & Ahituv, N. Modulating gene regulation to treat genetic disorders. *Nat. Rev. Drug Discov.* **19**, 757–
809 775 (2020).
810 18. Lalanne, J.-B. *et al.* Multiplex profiling of developmental enhancers with quantitative, single-cell expression
811 reporters. *bioRxiv* 2022.12.10.519236 (2022) doi:10.1101/2022.12.10.519236.
812 19. Maeder, M. L. *et al.* CRISPR RNA–guided activation of endogenous human genes. *Nat. Methods* **10**, 977–979
813 (2013).
814 20. Chavez, A. *et al.* Highly efficient Cas9-mediated transcriptional programming. *Nat. Methods* **12**, 326–328 (2015).
815 21. Esvelt, K. M. *et al.* Orthogonal Cas9 proteins for RNA-guided gene regulation and editing. *Nat. Methods* **10**, 1116–
816 1121 (2013).
817 22. Dixon, J. R. *et al.* Topological domains in mammalian genomes identified by analysis of chromatin interactions.
818 *Nature* vol. 485 376–380 Preprint at https://doi.org/10.1038/nature11082 (2012).
819 23. Satterstrom, F. K. *et al.* Large-Scale Exome Sequencing Study Implicates Both Developmental and Functional
820 Changes in the Neurobiology of Autism. *Cell* **180**, 568–584.e23 (2020).
821 24. Fu, J. M. *et al.* Rare coding variation provides insight into the genetic architecture and phenotypic context of
822 autism. *Nat. Genet.* **54**, 1320–1331 (2022).
823 25. Zhang, Y. *et al.* Rapid single-step induction of functional neurons from human pluripotent stem cells. *Neuron* **78**,
824 785–798 (2013).
825 26. Wang, C. *et al.* Scalable Production of iPSC-Derived Human Neurons to Identify Tau-Lowering Compounds by
826 High-Content Screening. *Stem Cell Reports* **9**, 1221–1233 (2017).
827 27. Lin, H.-C. *et al.* NGN2 induces diverse neuron types from human pluripotency. *Stem Cell Reports* **16**, 2118–2127
828 (2021).
829 28. Sanson, K. R. *et al.* Optimized libraries for CRISPR-Cas9 genetic screens with multiple modalities. *Nat. Commun.*
830 **9**, 5416 (2018).
831 29. Yao, D. *et al.* Multi-center integrated analysis of non-coding CRISPR screens. *bioRxiv* 2022.12.21.520137 (2022)
832 doi:10.1101/2022.12.21.520137.
833 30. Cao, J. *et al.* The single-cell transcriptional landscape of mammalian organogenesis. *Nature* **566**, 496–502 (2019).
834 31. Xu, Z., Sziraki, A., Lee, J., Zhou, W. & Cao, J. PerturbSci-Kinetics: Dissecting key regulators of transcriptome
835 kinetics through scalable single-cell RNA profiling of pooled CRISPR screens. *bioRxiv* 2023.01.29.526143 (2023)

836 doi:10.1101/2023.01.29.526143.
837 32. Song, M. *et al.* Mapping cis-regulatory chromatin contacts in neural cells links neuropsychiatric disorder risk
838 variants to target genes. *Nat. Genet.* **51**, 1252–1262 (2019).
839 33. McKenna, A. & Shendure, J. FlashFry: a fast and flexible tool for large-scale CRISPR target design. *BMC Biol.* **16**,
840 74 (2018).
841 34. Frankish, A. *et al.* GENCODE reference annotation for the human and mouse genomes. *Nucleic Acids Res.* **47**,
842 D766–D773 (2019).
843 35. Lizio, M. *et al.* Update of the FANTOM web resource: expansion to provide additional transcriptome atlases.
844 *Nucleic Acids Res.* **47**, D752–D758 (2019).
845 36. FANTOM Consortium and the RIKEN PMI and CLST (DGT) *et al.* A promoter-level mammalian expression atlas.
846 *Nature* **507**, 462–470 (2014).
847 37. Replogle, J. M. *et al.* Combinatorial single-cell CRISPR screens by direct guide RNA capture and targeted
848 sequencing. *Nat. Biotechnol.* **38**, 954–961 (2020).
849 38. Jerber, J., Haldane, J., Steer, J., Pearce, D. & Patel, M. Dissociation of neuronal culture to single cells for scRNA-
850 seq (10x Genomics) v1. Preprint at https://doi.org/10.17504/protocols.io.bh32j8qe.
851 39. Hao, Y. *et al.* Integrated analysis of multimodal single-cell data. *Cell* **184**, 3573–3587.e29 (2021).
852 40. Pagès, H. BSgenome: Software infrastructure for efficient representation of full genomes and their SNPs. *R*
853 *package version*.
854 41. Durinck, S., Spellman, P. T., Birney, E. & Huber, W. Mapping identifiers for the integration of genomic datasets
855 with the R/Bioconductor package biomaRt. *Nat. Protoc.* **4**, 1184–1191 (2009).
856 42. Durinck, S. *et al.* BioMart and Bioconductor: a powerful link between biological databases and microarray data
857 analysis. *Bioinformatics* **21**, 3439–3440 (2005).
858 43. Hahne, F. & Ivanek, R. Visualizing Genomic Data Using Gviz and Bioconductor. *Methods in Molecular Biology*
859 335–351 Preprint at https://doi.org/10.1007/978-1-4939-3578-9_16 (2016).
860 44. Rosenbloom, K. R. *et al.* ENCODE data in the UCSC Genome Browser: year 5 update. *Nucleic Acids Res.* **41**,
861 D56–63 (2013).
862 45. Li, H. *et al.* The Sequence Alignment/Map format and SAMtools. *Bioinformatics* **25**, 2078–2079 (2009).
863 46. Langmead, B. & Salzberg, S. L. Fast gapped-read alignment with Bowtie 2. *Nat. Methods* **9**, 357–359 (2012).